

TECHNICAL REPORT NUMBER 4

AN INVESTIGATION OF THE MUTUAL COUPLING EXISTING  
BETWEEN ARRAY ELEMENTS OF A THIRTY SIX  
ELEMENT ARRAY OF CROSSED SLOTS

Prepared by

ANTENNA RESEARCH LABORATORY

E. R. GRAF, PROJECT LEADER

March 4, 1966


CONTRACT NAS8-11251

GEORGE C. MARSHALL SPACE FLIGHT CENTER

NATIONAL AERONAUTICS AND SPACE ADMINISTRATION

HUNTSVILLE, ALABAMA

APPROVED BY



C. H. Holmes  
Head Professor  
Electrical Engineering

SUBMITTED BY



H. M. Summer  
Professor of  
Electrical Engineering

## FOREWORD

This is a technical report of a study conducted by the Electrical Engineering Department of Auburn University under the auspices of Auburn Research Foundation toward the fulfillment of the requirements prescribed in NASA Contract NAS8-11251.

## ABSTRACT

Electronically scanned antennas have become quite popular in recent years. These antennas usually consist of a large array of closely spaced elements. Due to the close spacing between the elements, coupling becomes important. Thus, one must examine the influence of mutual coupling in order to predict the feasibility of an electronic scanning array.

This report presents an analysis of the effects of mutual coupling on a 36 element, square array of crossed slots in an electrically large ground plane. The study was made by computing the mutual admittance between the slots and solving the simultaneous equations for a model array of parallel slots to obtain the terminal voltage and phase of each element. These parameters were tabulated for five representative pointings of the array.

Since the array pattern is proportional to the voltages along the slot, and the relative phase of each slot, it is a simple matter to calculate the array pattern with the aid of a computer. These patterns were plotted for the representative pointings, and coincide very closely to those in which mutual coupling was neglected.

The array gain was calculated for the various pointings. It was found to vary with direction of beam pointing, however, it does not

decrease by more than two decibels with respect to the array gain calculated with the mutual coupling neglected.

Therefore, one may conclude that the scanning capabilities of the 36 element array of crossed slots will not be seriously affected by mutual coupling between antenna elements.

TABLE OF CONTENTS

LIST OF TABLES.....	vi
LIST OF FIGURES.....	vii
I. INTRODUCTION.....	1
II. ANALYTICAL DEVELOPMENT.....	3
Mutual Impedance Between Dipoles	
Mutual Admittance Between Slots	
Method of Pattern Analysis	
III. ANALYTICAL EVALUATION.....	27
IV. CONCLUSIONS.....	40
BIBLIOGRAPHY.....	41
APPENDIX A.....	42
APPENDIX B.....	48
APPENDIX C.....	58

LIST OF TABLES

1.	The Power Gain of the Model Array With Respect to and Individual Element.....	34
A-1.	The Terminal Voltage and Admittance of the 36 Element Model Array of Parallel Slots For $L = 0$ and $M = 0$ .....	43
A-2.	The Terminal Voltage and Admittance of the 36 Element Model Array of Parallel Slots For $L = 0$ and $M = -7$ .....	44
A-3.	The Terminal Voltage and Admittance of the 36 Element Model Array of Parallel Slots For $L = -2$ and $M = -2$ .....	45
A-4.	The Terminal Voltage and Admittance of the 36 Element Model Array of Parallel Slots For $L = -3$ and $M = -4$ .....	46
A-5.	The Terminal Voltage and Admittance of the 36 Element Model Array of Parallel Slots For $L = -3$ and $M = -6$ .....	47

## LIST OF FIGURES

1.	A Half Wavelength Dipole.....	4
2.	A Two Element Array of Half Wavelength Dipoles.....	8
3.	A General Dipole Array Defining $r_{t1}$ , $r_{b1}$ , $r_{t2}$ and $r_{b2}$ .....	11
4.	A Half Wavelength Slot in an Electrically Large Ground Plane.....	14
5.	Four Element Array of Crossed Slots.....	22
6.	Model Array of Paralled Slots.....	23
7.	The Coordinate System of the Array Factor.....	25
8.	A 6 x 6 Array of Crossed Slots.....	29
9.	The Mutual Resistance Between Two Parallel Dipoles of Half Length $.250\lambda$ .....	39
B-1.	The Elevation Pattern for the 6 x 6 Model Antenna Array with $L = 0$ , $M = 0$ . ( $\phi = 90^\circ$ ).....	49
B-2.	The Elevation Pattern for the 6 x 6 Model Antenna Array with $L = 0$ , $M = -7$ . ( $\phi = 90^\circ$ ).....	50
B-3.	The Azimuth Array Pattern for the 6 x 6 Model Antenna Array with $L = 0$ , $M = -7$ . ( $\theta = 84^\circ$ ).....	51
B-4.	The Elevation Pattern for the 6 x 6 Model Antenna Array with $L = -2$ , $M = -2$ . ( $\phi = 45^\circ$ ).....	52
B-5.	The Aximuth Array Pattern for the 6 x 6 Model Antenna Array with $L = -2$ , $M = -2$ . ( $\phi = 24^\circ$ ).....	53

B-6.	The Elevation Pattern for the 6 x 6 Model Antenna Array with L = -3, M = -4. ( $\phi = 53^\circ$ ).....	54
B-7.	The Aximuth Array Pattern for the 6 x 6 Model Antenna Array with L = -3, M = -4. ( $\theta = 45^\circ$ ).....	55
B-8.	The Elevation Pattern for the 6 x 6 Model Antenna Array with L = -3, M = -6. ( $\phi = 63^\circ$ ).....	56
B-9.	The Azimuth Array Pattern for the 6 x 6 Model Antenna Array with L = -3, M = -6. ( $\theta = 72^\circ$ ).....	57



## I. INTRODUCTION

W. F. Hayes, J. D. Tillman, E. R. Graf

Tracking antennas used in conjunction with space vehicles and artificial earth satellites have become quite important in recent years. Often a scanned parabolic dish antenna is used for this purpose. The narrow beam may be shifted by moving the dish. This and similar techniques accomplish the task but have the disadvantage of requiring the usually large mass of the antenna to be mechanically moved by electric motors.

In recent years, electronic scanning antennas have been used successfully. These do not require the movement of the antenna nor the presence of an operator. The antenna consists of a number of identical elements in which the beam is shifted by varying the input phase or amplitude to the individual elements. The field pattern is obtained by multiplication of the pattern of each individual element and that of the array in which the elements are located.

Since the beam is to be moved through the entire hemisphere it is desirable for each element to have a hemispherical radiation pattern. This prevents the field maximum from varying as the beam is scanned through the hemisphere.

The object of this report is to evaluate the usefulness of a 36 element square array, using crossed slots for array elements, as an

electronically scanned tracking antenna. The crossed slot produces a nearly hemispherical pattern and the resultant beam may be scanned through the entire hemisphere by means of thirty five digital phase shifters. These are capable of shifting phase in  $22.5^\circ$  increments from  $0^\circ$  to  $360^\circ$ . The position of the beam for each phase variation may easily be determined by neglecting the effects of mutual coupling and plotting the array pattern. Since the elements are closely spaced it is obvious that the array elements are coupled; therefore, it becomes necessary to examine the effects of mutual coupling on the array pattern and gain. This is accomplished by calculating the mutual admittance between each element and setting up the linear simultaneous equations to yield the actual voltage magnitude and phase incident upon each element. Having solved these equations the array pattern, including the effects of mutual coupling, is plotted and compared to that of the theoretical pattern for uncoupled elements.

## II. ANALYTICAL DEVELOPMENT

### Mutual Impedance Between Dipoles

Since the slot is the dual of a dipole it is advantageous to derive the mutual impedance between dipoles and, using the duality principle, obtain an expression for the mutual admittance between slots.

In order to arrive at an expression for the mutual impedance between dipoles, first consider the self impedance of a single dipole as shown in Figure 1. Assuming a sinusoidal current distribution  $I(z) = I_T \cos(kz)$ , the complex power to the antenna is given by

$$P_c = \frac{1}{2} [V_T I_T^*] \quad (1)$$

or

$$P_c = \frac{1}{2} I_T I_T^* Z_T, \quad (2)$$

where  $Z_T$  is the terminal impedance of the dipole. The complex input power may also be expressed as the integral of the average complex Poynting vector,  $\langle \bar{s} \rangle_p$ , over the surface, this may be written

$$P_c = \int \langle \bar{s} \rangle_p \cdot \bar{da} \quad (3)$$

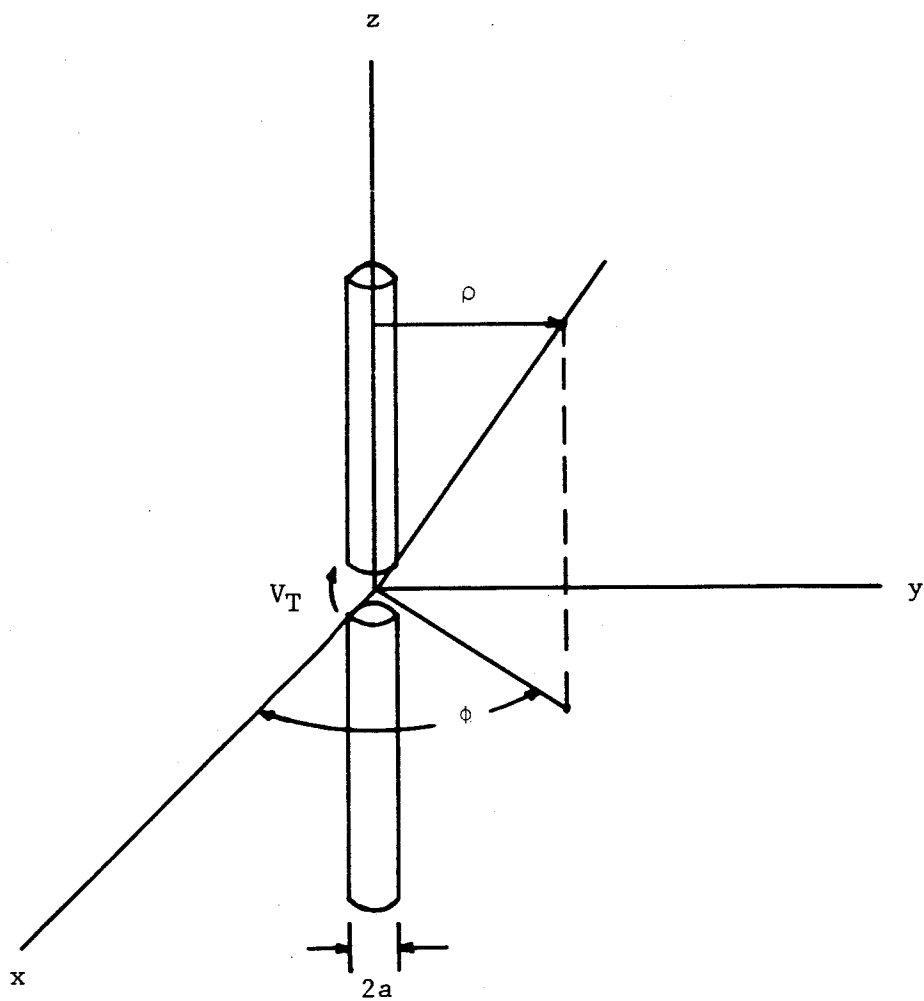


Fig. 1--A half wavelength dipole

where

$$\langle \bar{s} \rangle_p = \frac{1}{2} \bar{E} \times \bar{H}^* \quad (4)$$

At the surface of the dipole the average Poynting vector becomes

$$\langle \bar{s} \rangle_p = -\frac{1}{2} E_z H_\phi^* \bar{a}_\rho \quad (5)$$

From Ampere's law

$$\oint \bar{H} \cdot d\bar{\ell} = I \quad (6)$$

Taking a closed contour around the surface of the dipole yields

$$\int_0^{2\pi} H_\phi(z) a d\phi = I_z(z), \quad (7)$$

thus,

$$H_\phi(z) = \frac{I_T \cos(kz)}{2\pi a} \quad (8)$$

Substituting (8) into (5) yields

$$\langle \bar{s} \rangle_p = -\frac{E_z(z) I_T^* \cos(kz)}{4\pi a} \bar{a}_\rho \quad (9)$$

at the surface of the dipole.

Using equation (3) and (9), the complex power is given by

$$P_c = -\int \frac{E_z(z) I_T^* \cos(kz)}{4\pi a} da \quad (10)$$

Evaluating  $E_z(z)$  at the surface of the dipole yields

$$P_c = - \int_{-\lambda/4}^{\lambda/4} \int_0^{2\pi} \frac{E_z(z) I_T^* \cos(kz)}{4\pi a} a d\phi dz \quad (11)$$

or

$$P_c = - \frac{I_T^*}{2} \int_{-\lambda/4}^{\lambda/4} E_z(z) \cos(kz) dz \quad (12)$$

for the complex power.

Comparing equation (12) to (2) the impedance of the dipole is immediately obtained as

$$Z_T = - \frac{1}{I_T} \int_{-\lambda/4}^{\lambda/4} E_z(z) \cos(kz) dz. \quad (13)$$

If  $a \rightarrow 0$ , the electric field intensity is given by

$$E_z(z) = -j \frac{I_T \eta}{4\pi} \left[ \frac{e^{-jkr_{t1}}}{r_{t1}} + \frac{e^{-jkr_{b1}}}{r_{b1}} \right] l \quad (14)$$

where  $r_{t1} = \lambda/4 - z$ ,  $r_{b1} = \lambda/4 + z$  and  $\eta$  is the intrinsic impedance of free space. The expression for the terminal impedance of a dipole then becomes

$$Z_T = \frac{j\eta}{4\pi} \int_{-\lambda/4}^{\lambda/4} \left[ \frac{e^{-jkr_{t1}}}{r_{t1}} + \frac{e^{-jkr_{b1}}}{r_{b1}} \right] \cos(kz) dz. \quad (15)$$

Consider two coupled dipoles as shown in Figure 2. Again assume a sinusoidal current distribution along the half wave length antennas. Let the radius of each dipole approach zero and assume identical dipoles such that  $Z_{11} = Z_{22}$  and  $Z_{12} = Z_{21}$ . Since the system is linear the relationship between the currents and voltages may be represented by the following simultaneous equations:

$$V_1 = I_1 Z_{11} + I_2 Z_{12}$$

and (16)

$$V_2 = I_1 Z_{21} + I_2 Z_{22}.$$

Letting  $V_1 = V_2 = V_s$ , yields  $I_1 = I_2 = I_s$ . Solving the simultaneous equations one obtains

$$V_s = I_s (Z_{11} + Z_{12}), \quad (17)$$

or

$$V_s = I_s Z_s, \quad (18)$$

where the symmetrical impedance,  $Z_s$ , is given by

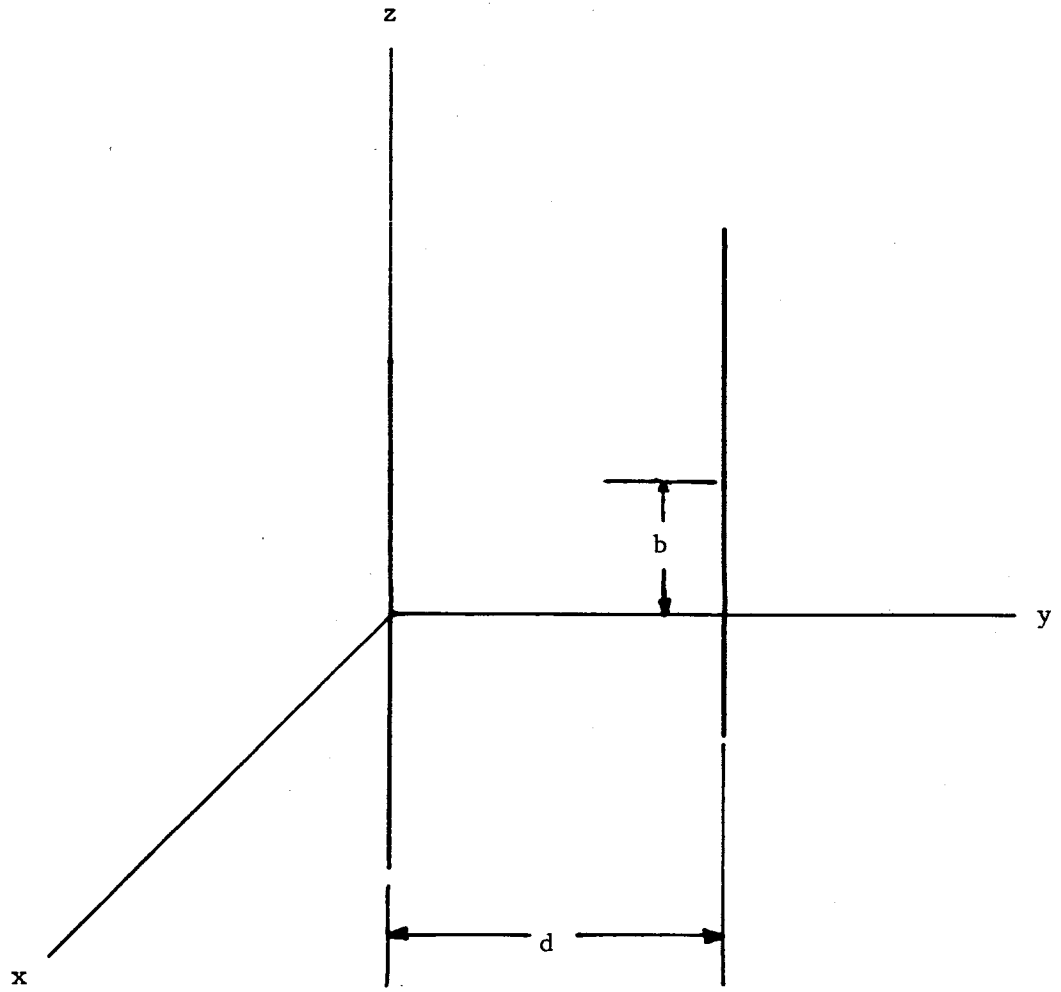


Fig. 2--A two element array of half-wavelength dipoles



$$Z_s = Z_{11} + Z_{12}. \quad (19)$$

In a similar manner letting  $V_1 = -V_2 = V_a$ , and thus  $I_1 = -I_2 = I_a$ , equation (16) yields

$$V_a = I_a Z_a, \quad (20)$$

where the antisymmetrical impedance,  $Z_a$ , is given by

$$Z_a = Z_{11} - Z_{12}. \quad (21)$$

Simultaneous solution of equations (19) and (21) gives the mutual impedance between the two dipoles in terms of the symmetrical and antisymmetrical impedances as

$$Z_{12} = \frac{1}{2} (Z_s - Z_a). \quad (22)$$

Obviously  $Z_s$  is the isolated impedance of each dipole when they are fed identically. From (13) one obtains

$$Z_s = -\frac{1}{I_s} \int_{-\lambda/4}^{\lambda/4} E_z(z) \cos(kz) dz, \quad (23)$$

where  $E_z(z)$  is due to the currents on both antennas. This electric field intensity is given by

$$E_z(z) = -j \frac{\eta I_s}{4\pi} \left[ \frac{e^{-jkr_{t1}}}{r_{t1}} + \frac{e^{-jkr_{b1}}}{r_{b1}} + \frac{e^{-jkr_{t2}}}{r_{t2}} + \frac{e^{-jkr_{b2}}}{r_{b2}} \right] \quad (24)$$

where  $r_{t1}$ ,  $r_{t2}$ ,  $r_{b1}$ , and  $r_{b2}$  are defined in Figure 3. For parallel dipoles, these quantities are given by

$$\begin{aligned} r_{t1} &= \lambda/4 - z \\ r_{b1} &= \lambda/4 - z \\ r_{t2} &= \sqrt{d^2 + (b + \lambda/4 - z)^2}, \\ r_{b2} &= \sqrt{d^2 + (b - \lambda/4 - z)^2}. \end{aligned} \quad (25)$$

Inserting  $E_z(z)$  into  $Z_s$  the symmetrical impedance becomes

$$\begin{aligned} Z_s &= j \frac{\eta}{4\pi} \int_{-\lambda/4}^{\lambda/4} \left[ \frac{e^{-jkr_{t1}}}{r_{t1}} + \frac{e^{-jkr_{b1}}}{r_{b1}} \right] \cos(kz) dz \\ &+ j \frac{\eta}{4\pi} \int_{-\lambda/4}^{\lambda/4} \left[ \frac{e^{-jkr_{t2}}}{r_{t2}} + \frac{e^{-jkr_{b2}}}{r_{b2}} \right] \cos(kz) dz. \end{aligned} \quad (26)$$

Following the same procedure the antisymmetrical impedance becomes

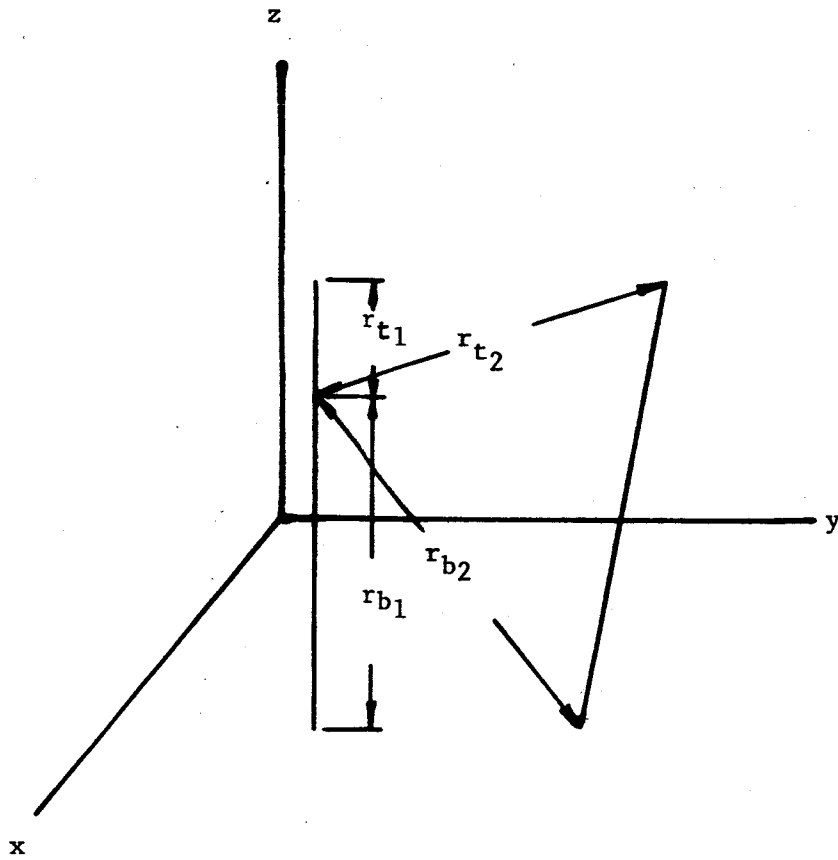


Fig. 3--A general dipole array defining  $r_{t1}$ ,  $r_{b1}$ ,  $r_{t2}$  and  $r_{b2}$ .

$$\begin{aligned}
 Z_a = j \frac{\eta}{4\pi} \int_{-\lambda/4}^{\lambda/4} \left[ \frac{e^{-jkr_{t1}}}{r_{t1}} + \frac{e^{-jkr_{b1}}}{r_{b1}} \right] \cos(kz) dz \\
 - j \frac{\eta}{4\pi} \int_{-\lambda/4}^{\lambda/4} \left[ \frac{e^{-jkr_{t2}}}{r_{t2}} + \frac{e^{-jkr_{b2}}}{r_{b2}} \right] \cos(kz) dz.
 \end{aligned} \tag{27}$$

Substitution of (26) and (27) into (22) yields

$$Z_{12} = j \frac{\eta}{4\pi} \int_{-\lambda/4}^{\lambda/4} \left[ \frac{e^{-jkr_{t2}}}{r_{t2}} + \frac{e^{-jkr_{b2}}}{r_{b2}} \right] \cos(kz) dz. \tag{28}$$

This is the desired expression for the mutual impedance between dipoles.

#### Mutual Admittance Between Slot-Antennas

Having derived the mutual impedance between dipoles the duality principle may be used to obtain the mutual admittance between parallel slots in an infinite ground plane. The duality principle between slots and dipoles may be stated as follows:

If an e.m.f. of frequency  $f$  is applied to an ideal slot antenna from an arbitrary source, the electromagnetic field vectors  $\bar{E}$  and  $\bar{H}$  in the slot and the space surrounding the slot will have the same directions and will be the same functions of the space co-ordinates as

the directions and the functions of the vectors  $\bar{H}$  and  $\bar{E}$ , respectively, of the electromagnetic field of a dipole consisting of an ideally-conducting, infinitely thin plate, located in free space and having the same shape and dimensions as the slot when an e.m.f. of the same frequency is applied to the plate at corresponding points.<sup>2</sup>

The duality principle allows one to obtain an expression for  $H_z$  as given below

$$H_z = -j \frac{V}{2\pi\eta} \left[ \frac{e^{-jkr_{t1}}}{r_{t1}} + \frac{e^{-jkr_{b1}}}{r_{b1}} \right], \quad (29)$$

where  $r_{t1}$  and  $r_{b1}$  are the same as that in the dipole solution. One observes that this is explicitly true only if the slot and dipole have the same geometric shape. However, in this case a cylindrical dipole is assumed to be the dual of a rectangular slot. In addition both the slot and the dipole have been assumed infinitely thin. Both of these assumptions introduce little error and may be neglected.

The mutual admittance between slots may be obtained by the method used to obtain the mutual impedance between dipoles. Thus, it is again necessary to first obtain the self admittance of a single slot and use that to obtain the mutual admittance between coupled slot antennas.

Assuming a sinusoidal voltage distribution along the slot shown in Figure 4 the electric field intensity in the slot is given by

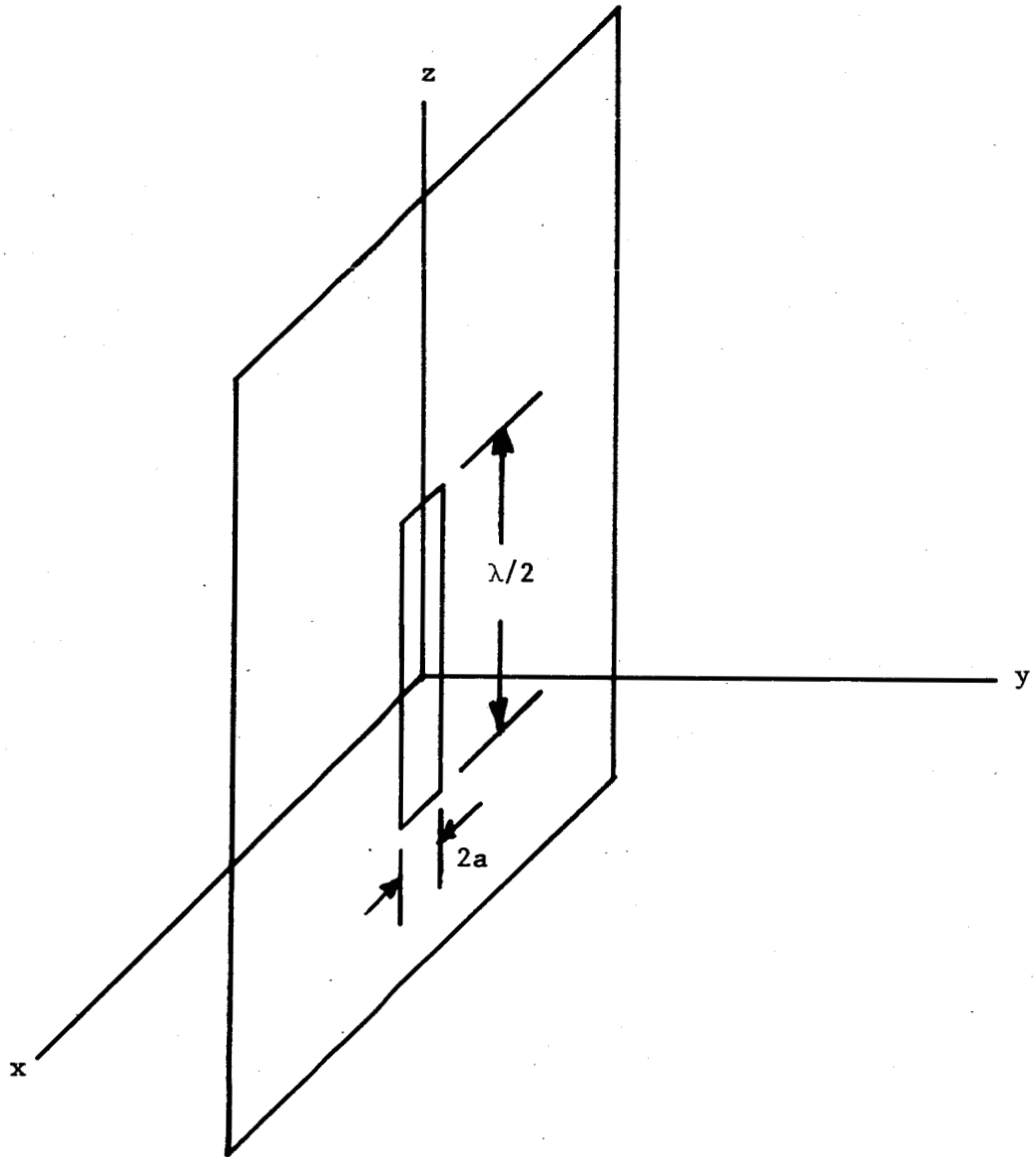


Fig. 4--A half wavelength slot in an electrically large ground plane.

$$E_x(z) = \frac{V}{2a} \cos(kz), \quad (30)$$

where  $V$  is the terminal voltage of the slot. Now the average complex power becomes

$$\langle \bar{s} \rangle_p = 1/2 \bar{E} \times \bar{H}^* = -1/2 E_x H_z^* \bar{n}, \quad (31)$$

where  $\bar{n}$  is normal to and directed outward from the plane of the slot.

Equation (31) may also be written

$$\langle \bar{s} \rangle_p = -\frac{V}{4a} \cos(kz) H_z^*(z) \bar{n} \quad (32)$$

Integrating (32) over the total surface of the slot the complex power is given as

$$P_c = -V \int_{-\lambda/4}^{\lambda/4} H_z^*(z) \cos(kz) dz. \quad (33)$$

If the slot is cavity backed, the complex power is halved due to the halving of the physical aperture, thus

$$P_c = -\frac{V}{2} \int_{-\lambda/4}^{\lambda/4} H_z^*(z) \cos(kz) dz. \quad (34)$$

The complex power may also be expressed as

$$P_c = 1/2 V_T V_T^* Y_T. \quad (35)$$

Combination of (34) and (35) yields

$$Y_T = -\frac{1}{V} \int_{-\lambda/4}^{\lambda/4} H_z(z) \cos(kz) dz \quad (36)$$

and by substituting (29) into the above expression the self admittance of a cavity backed slot may be written as

$$Y_T = \frac{j}{2\pi\eta} \int_{-\lambda/4}^{\lambda/4} \left[ \frac{e^{-jkr_{t1}}}{r_{t1}} + \frac{e^{-jkr_{b1}}}{r_{b1}} \right] \cos(kz) dz. \quad (37)$$

For the case of two coupled slots the linear simultaneous equations are

$$I_1 = Y_{11}V_1 + Y_{12}V_2 \quad (38)$$

$$I_2 = Y_{12}V_1 + Y_{22}V_2.$$

Again the use of symmetrical and antisymmetrical inputs yields

$$Y_s = Y_{11} + Y_{12}$$

and

$$Y_a = Y_{11} - Y_{12} \quad (39)$$



and thus

$$Y_{12} = 1/2(Y_s - Y_a) . \quad (40)$$

It is obvious that  $Y_s$  is the isolated admittance of each slot when symmetrically fed. From equation (36)

$$Y_s = -\frac{1}{V_s} \int_{-\lambda/4}^{\lambda/4} H_z(z) \cos(kz) dz. \quad (41)$$

$H_z(z)$  is due to the voltages along each slot antenna and is given by

$$H_z(z) = -\frac{jV_s}{2\pi\eta} \left[ \frac{e^{-jkr_{t1}}}{r_{t1}} + \frac{e^{-jkr_{b1}}}{r_{b1}} + \frac{e^{-jkr_{t2}}}{r_{t2}} + \frac{e^{-jkr_{b2}}}{r_{b2}} \right]. \quad (42)$$

The quantities  $r_{t1}$ ,  $r_{t2}$ ,  $r_{b1}$ , and  $r_{b2}$  are the same as those for the dipole solution and are shown in Figure 3. Inserting  $H_z(z)$  into  $Y_s$  the symmetrical admittance is given by

$$Y_s = \frac{j}{2\pi\eta} \int_{-\lambda/4}^{\lambda/4} \left[ \frac{e^{-jkr_{t1}}}{r_{t1}} + \frac{e^{-jkr_{b1}}}{r_{b1}} \right] \cos(kz) dz \quad (43)$$

$$+ \frac{j}{2\pi\eta} \int_{-\lambda/4}^{\lambda/4} \left[ \frac{e^{-jkr_{t2}}}{r_{t2}} + \frac{e^{-jkr_{b2}}}{r_{b2}} \right] \cos(kz) dz.$$

Similarly, the antisymmetrical admittance may be obtained and used in (40) to yield

$$Y_{12} = \frac{j}{2\eta\pi} \int_{-\lambda/4}^{\lambda/4} \left[ \frac{e^{-jkr_{t2}}}{r_{t2}} + \frac{e^{-jkr_{b2}}}{r_{b2}} \right] \cos(kz) dz. \quad (44)$$

Equation (44) gives a general expression for the mutual admittance between cavity backed half wave length slots. It is obvious that equation (44) will be valid for any slot length if the integration limits are altered accordingly. Also, by comparing (28) and (44) one notices that the mutual admittance between slots takes the same form as the mutual impedance between dipole antennas. This implies that any general results obtained by employing crossed slot elements in the array will hold equally well if crossed dipoles are used as antenna elements.

#### Method of Pattern Analysis

In an attempt to analyze the effects of mutual coupling on the field pattern and gain of the array, one must first know the value of the mutual admittances. As has been shown, the expression for the mutual admittance is given by

$$Y_{12} = \frac{j}{2\eta\pi} \int_{-\lambda/4}^{\lambda/4} \left[ \frac{e^{-jkr_{t2}}}{r_{t2}} + \frac{e^{-jkr_{b2}}}{r_{b2}} \right] \cos(kz) dz$$

where  $r_{t2}$  and  $r_{b2}$  are shown in Figure 3. Obviously the integral cannot be directly evaluated. It becomes necessary to change the expression to a more useful form. By Euler's identity

$$e^{-jkr_{t2}} = \cos(kr_{t2}) - j\sin(kr_{t2})$$

and

$$e^{-jkr_{b2}} = \cos(kr_{b2}) - j\sin(kr_{b2}).$$

(45)

Making these substitutions the mutual admittance becomes

$$Y_{12} = \frac{j}{2\eta\pi} \int_{-\lambda/4}^{\lambda/4} \left[ \frac{\cos(kr_{t2})}{r_{t2}} + \frac{\cos(kr_{b2})}{r_{b2}} \right] \cos(kz) dz$$

$$+ \frac{1}{2\eta\pi} \int_{-\lambda/4}^{\lambda/4} \left[ \frac{\sin(kr_{t2})}{r_{t2}} + \frac{\sin(kr_{b2})}{r_{b2}} \right] \cos(kz) dz.$$

(46)

Although the expression for the mutual admittance still may not be integrated by straightforward means, it may easily be numerically integrated by a computer with Simpson's 1/3 rule of integration. Simpson's rule may be expressed as follows:

$$\int_a^b f(z) dz = \frac{b-a}{3n} \left[ f(a) + 4f(z_1) + 2f(z_2) + \dots + 4f(z_{n-1}) + f(b) \right]$$

(47)

where  $n$  is always even and is the number of subintervals in the interval from  $a$  to  $b$ . The accuracy is dependent upon the number of subintervals chosen and is increased as  $n$  is increased.

After determining the mutual admittance the next step is to examine the simultaneous equations representing the voltage and current relationships of the slots. To analyze the affects of mutual coupling on the array pattern, constant current inputs may be assumed and the simultaneous equations solved to obtain the terminal voltage of each slot. For the  $6 \times 6$  array of crossed slots, 72 simultaneous equations must be solved for the 72 voltages. Clearly one would not wish to solve these equations without a computer. It is therefore necessary to change the simultaneous equations into a form which may readily be solved using computer techniques.

Consider the equations representing two slots, namely

$$I_1 = Y_{11}V_1 + Y_{12}V_2$$

and

$$I_2 = Y_{21}V_1 + Y_{22}V_2.$$

(48)

Since  $I$ ,  $Y$ , and  $V$  are complex numbers it is necessary to separate the real part from the imaginary.

$$(I_{1R} + jI_{1Q}) = (G_{11} + jB_{11})(V_{1R} + jV_{1Q}) + (G_{12} + jB_{12})(V_{2R} + jV_{2Q})$$

(49)

$$(I_{2R} + jI_{2Q}) = (G_{21} + jB_{21})(V_{1R} + jV_{1Q}) + (G_{22} + jB_{22})(V_{2R} + jV_{2Q})$$

Expanding these equations and setting the real parts equal and the imaginary parts equal yields

$$\begin{aligned}
 I_{1R} &= G_{11}V_{1R} - B_{11}V_{1Q} + G_{12}V_{2R} - B_{12}V_{2Q} \\
 I_{1Q} &= B_{11}V_{1R} + G_{11}V_{1Q} + B_{12}V_{2R} + G_{12}V_{2Q} \\
 I_{2R} &= G_{21}V_{1R} - B_{21}V_{1Q} + G_{22}V_{2R} - B_{22}V_{2Q} \\
 I_{2Q} &= B_{21}V_{1R} + G_{21}V_{1Q} + B_{22}V_{2R} + G_{22}V_{2Q}
 \end{aligned}
 \tag{50}$$

These equations may be changed to matrix form as

$$\begin{bmatrix} I_{1R} \\ I_{1Q} \\ I_{2R} \\ I_{2Q} \end{bmatrix} = \begin{bmatrix} G_{11} & -B_{11} & G_{12} & -B_{12} \\ B_{11} & G_{11} & B_{12} & G_{12} \\ G_{21} & -B_{21} & G_{22} & -B_{22} \\ B_{21} & G_{21} & B_{22} & G_{22} \end{bmatrix} \begin{bmatrix} V_{1R} \\ V_{1Q} \\ V_{2R} \\ V_{2Q} \end{bmatrix}
 \tag{51}$$

The simultaneous equations represented by matrix equation (51) may easily be solved on a computer by inverting the augmented matrix. Due to limited computer memory and accumulated round off error the computer available will not invert a matrix larger than 90 x 90. For the thirty six element array of crossed-slots the resulting matrix is 144 x 144, thus some approximations must be made in order to reduce the size of the matrix. To make this reduction, consider four elements

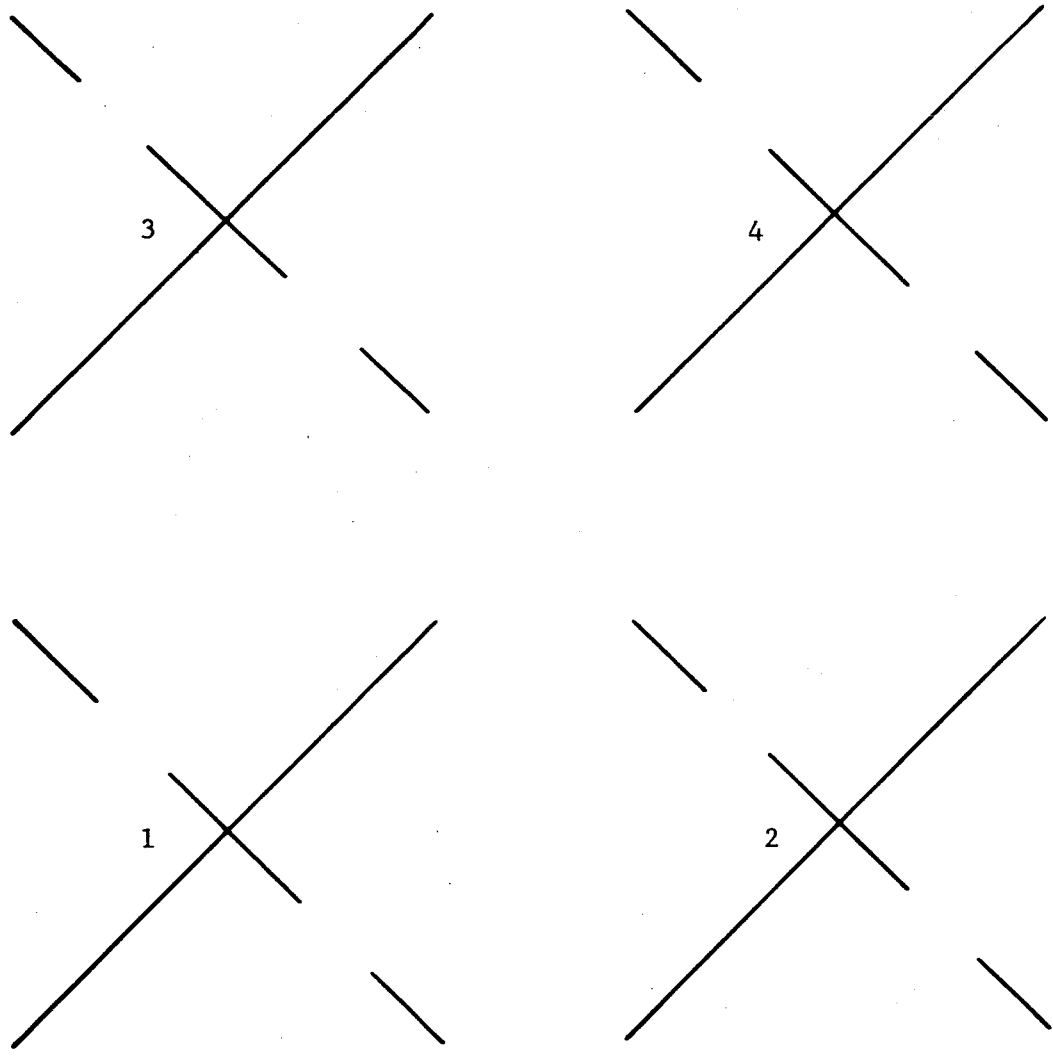


Fig. 5--Four Element Array of Crossed Slots

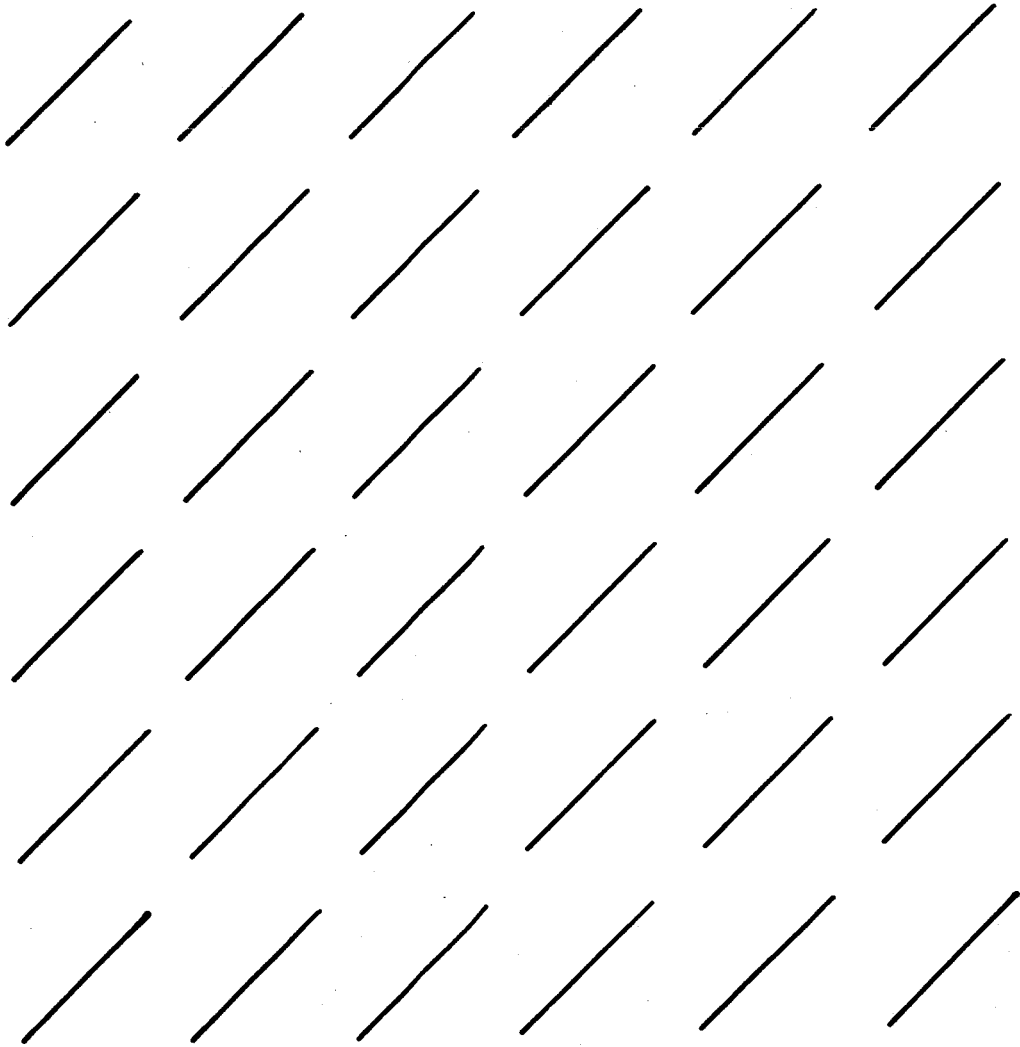


Fig. 6--Model Array of parallel slots

of the array as shown in Figure 5. First examine the mutual coupling between the slot indicated by the solid line of element one and each other element. The coupling due to the slot indicated by the dashed line of element one is zero. Also the coupling due to each perpendicular (dashed line) slot is negligible when compared to the coupling of each corresponding parallel (solid line) slot. A valid model, consisting only of parallel slots, may thus be used in obtaining the array pattern. The simultaneous equations representing the model of parallel slots form a 72 x 72 matrix, which may be solved to yield the terminal voltage of each slot.

The field pattern for an array of identical elements is given by the product of the field pattern produced by a single element and the array factor. The field pattern for an array of slots may be written as

$$E(\theta, \phi) = Kf(\theta, \phi) \sum_{i=1}^N v_i e^{jk(r - r_i)}. \quad (52)$$

The normalized field pattern of each individual source is  $f(\theta, \phi)$  and  $N$  is the number of elements in the array. The distance  $r_i$ , may be determined by geometrical means from Figure 7 as

$$r_i = r - x_i \sin \theta \cos \phi - y_i \sin \theta \sin \phi - z_i \cos \theta. \quad (53)$$



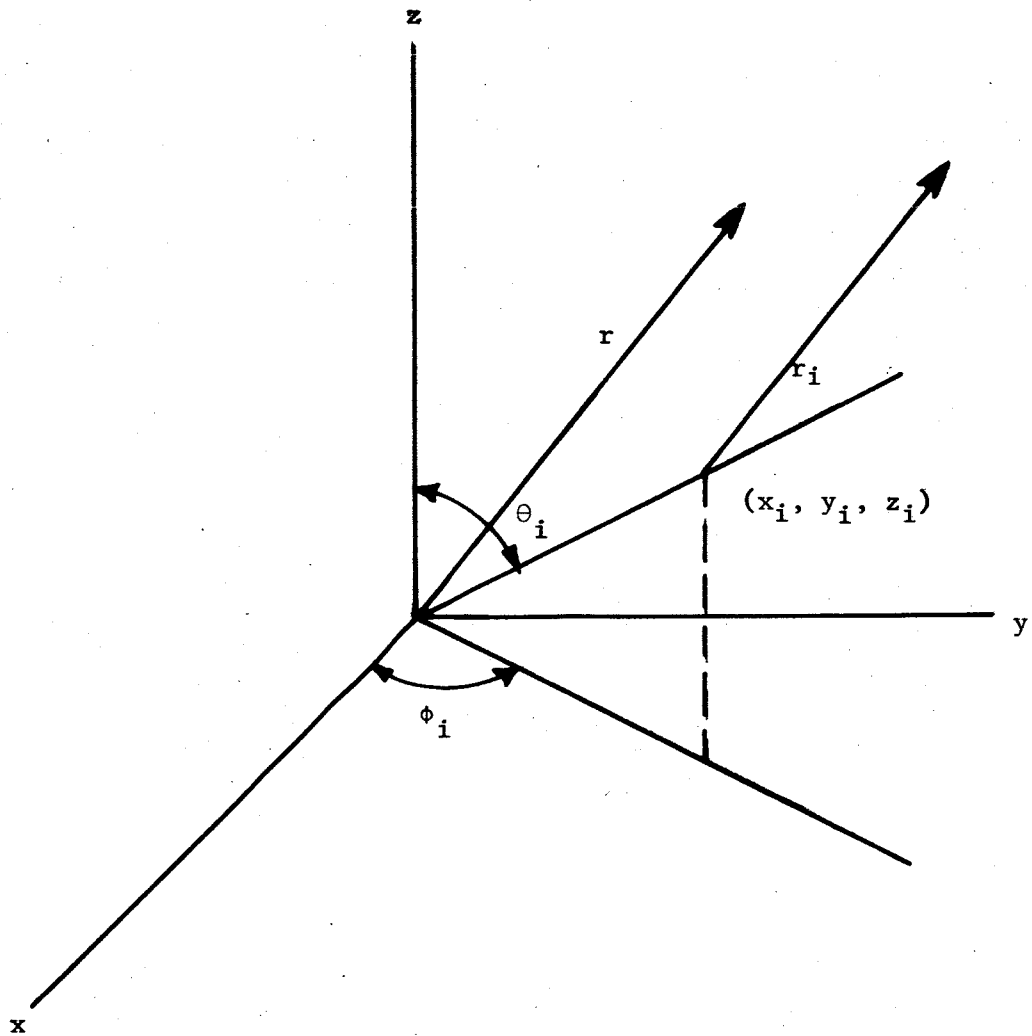


Fig. 7--The coordinate system of the array factor.

The calculated input voltages to the slots may be of unequal magnitude and relative phase, so the array factor must contain the weighting function,  $V_i$ . Thus, the array factor becomes

$$F(\theta, \phi) = \sum_{i=1}^N V_i e^{jk(r - r_i)}. \quad (54)$$

Using (54), the array factor for any configuration of parallel slots may be obtained.

### III. ANALYTICAL EVALUATION

An analytical method has been established for evaluating the effect of mutual coupling on the pattern of any array containing dipoles or slots, in particular, an array containing 36 crossed slots. Now one must merely carry out the numerical operations in order to obtain the array pattern with the effects of mutual coupling included. Obviously these effects will vary with beam position, so if a total analysis were to be conducted one would have to analyze each pointing of the array. The antenna, however, is to scan the entire hemisphere, therefore, it is impractical to examine each beam position. This indicates that a representative set of beam positions must be chosen and studied to yield a reasonable evaluation.

The most representative set of beam locations includes the one most affected and the one least affected by mutual coupling, and a few between these extremes. Obviously, the vertical position will be least affected since no input phase variation is required about the center of the array. To obtain the other extreme, one should choose the pointing which exhibits the most unsymmetrical phase distribution. This occurs near the horizon along the diagonal of the array. These positions were analyzed along with three other pointings.

The input phase to the  $pq^{\text{th}}$  element of the array, where  $p$  designates the row and  $q$  the column, is given by

$$\delta_{pq} = (pM + qL) 22.5^\circ. \quad (55)$$

$M$  and  $L$  may be any integer greater than or equal to  $-7$  and less than or equal to  $7$ , where  $\sqrt{L^2 + M^2}$  is less than  $7$ . Each beam position of the array may be completely defined by  $L$  and  $M$ . For clarity the various pointings of the array to be analyzed will be referred to by their values of  $L$  and  $M$ . These values for the five representative pointings are as follows:

$L = 0$	$M = 0$	Theoretical Maximum at $\phi = 0^\circ$ and $\theta = 0^\circ$
$L = 0$	$M = -7$	Theoretical Maximum at $\phi = 90^\circ$ and $\theta = 84^\circ$
$L = -2$	$M = -2$	Theoretical Maximum at $\phi = 45^\circ$ and $\theta = 24^\circ$
$L = -3$	$M = -4$	Theoretical Maximum at $\phi = 53^\circ$ and $\theta = 45^\circ$
$L = -3$	$M = -6$	Theoretical Maximum at $\phi = 63^\circ$ and $\theta = 72^\circ$

where  $\theta$  and  $\phi$  are shown in Figure 8.

With the aid of a computer the voltage to each slot has been calculated assuming an arbitrary magnitude for the input current of .25 ma. These voltages along with the input admittance to each element are tabulated in Appendix A for five beam positions. With

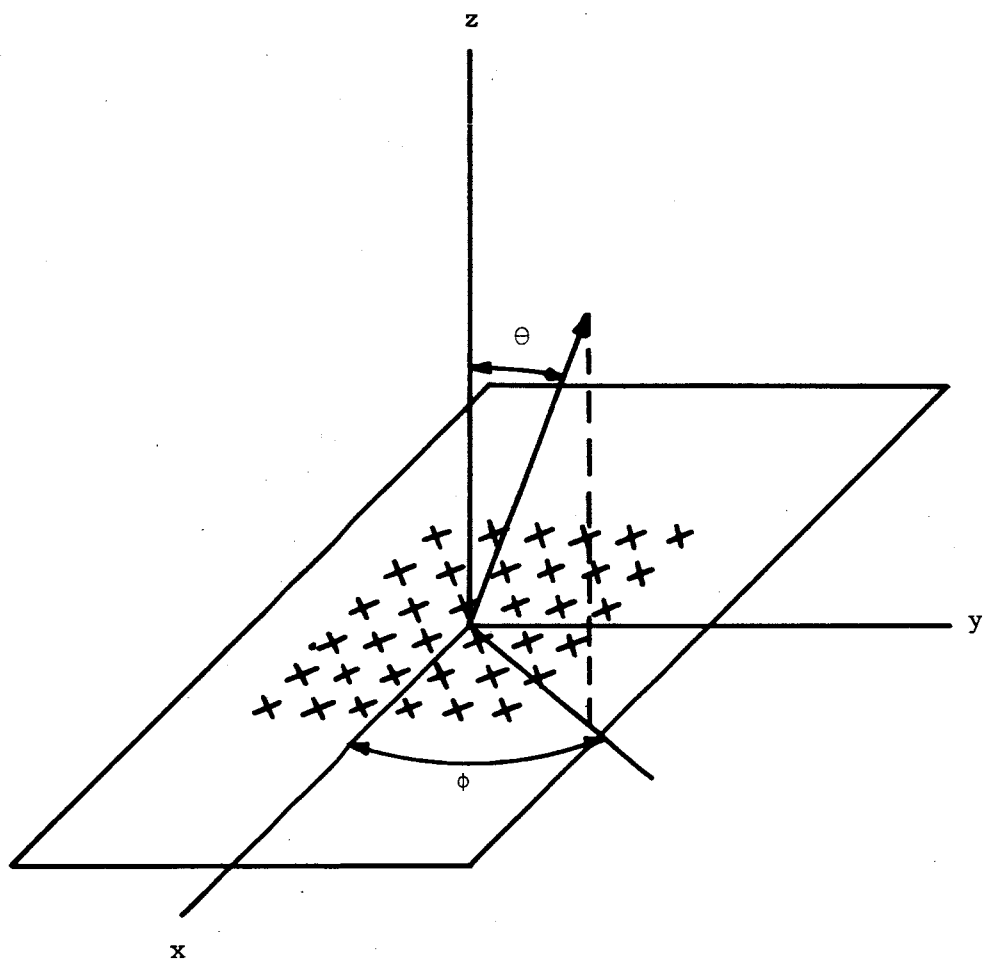


Fig. 8--A 6 x 6 array of crossed slots.

no mutual coupling the input admittance would obviously be that of an isolated element and is

$$Y_{11} = [1.029 + j.599] \text{ mmhos}$$

or

$$Y_{11} = 1.19 \angle 30.2^\circ \text{ mmhos.}$$

Comparing the above value of input admittance to those tabulated in Appendix A indicates the magnitude and phase of the terminal admittance has been affected in each case.

The voltage of each slot, neglecting mutual coupling, may be given by

$$V_{pq} = I_{pq} / Y_{11}, \quad (56)$$

where  $V_{pq}$  and  $I_{pq}$  are the voltage and current to the  $pq^{\text{th}}$  element.

Now

$$I_{pq} = .25 \angle \delta_{pq} \text{ ma,}$$

therefore

$$V_{pq} = .210 \angle \delta_{pq} - 30.2^\circ \text{ volts.}$$

Comparing this voltage to the tabulated values, the affect of mutual coupling is evident. Even though the voltages have been significantly altered, no conclusions may be made concerning the overall effect of the coupling on the pattern and gain of the array at this point.

Using the tabulated voltages the array pattern may be obtained from (54). These patterns are shown for each pointing with and without the affects of mutual coupling in Appendix B. The position of the field maximum in these patterns is not altered significantly by the coupling. The magnitude of the beam has been significantly altered in several cases. It has been decreased in most cases, but for  $L = -3, M = -4$  and  $L = -3, M = -6$  the magnitude is increased; however, the shape of the theoretical pattern has been maintained in each case.

The magnitude of the beam influences the gain of the array necessitating the evaluation of the array power gain for each representative pointing. It is a simple matter to find the total input power to the array since the input voltage and terminal admittance of each slot is known. The total input power to the array may be expressed as

$$P_T = \operatorname{Re} \sum_{p=0}^5 \sum_{q=0}^5 |V_{pq}|^2 Y_{pq}$$

or

$$P_T = \sum_{p=0}^5 \sum_{q=0}^5 |V_{pq}|^2 G_{pq}$$

(57)

where  $G_{pq}$  is the real part of the terminal admittance of the  $pq^{\text{th}}$  element. Therefore, the power gain of the array may be obtained for each pointing using any desired reference. Choosing a single slot in an infinite ground plane as a reference, one arrives at the expression for the reference power;

$$P_{\text{ref}} = |V|^2 G_{11}. \quad (58)$$

$G_{11}$  is the real part of the input admittance to a single isolated half wavelength slot. The reference power is the power input to the reference antenna necessary to yield the same field maximum as the array. The weighted array factor, (54), of a single slot is equal to the input voltage to the slot. Therefore, the reference power becomes

$$P_{\text{ref}} = |F(\theta, \phi)_{\text{max}}|^2 G_{11}, \quad (59)$$

where  $F(\theta, \phi)_{\text{max}}$  is the maximum value of the weighted array factor.

Thus, the power gain of the array becomes

$$G = P_{\text{ref}}/P_T \quad (60)$$

or

$$G = |F(\theta, \phi)_{\text{max}}|^2 G_{11}/P_T$$



Having the above expression for power gain, the gain of the array with no mutual coupling included may be derived. To obtain this gain, let  $V_s$  be the magnitude of the input voltage to each slot. The array pattern maximum may be obtained from (54) and equals  $36 V_s$ . Thus, the reference power becomes

$$P_{\text{ref}} = |36 V_s|^2 G_{11}.$$

The total power to the array may be obtained by summing the input power to the slots to yield,

$$P_T = 36 V_s^2 G_{11}.$$

Therefore, the array gain, neglecting mutual coupling, is 36.

The array gain with mutual coupling included is tabulated in Table 1, it is seen to vary for different beam positions. This variation is expected, but when mutual coupling is included one generally expects the gain to decrease, as is the case for three of the pointings. However, two calculated pointings gave gains greater than that of the idealized array. In these cases mutual coupling has actually improved the array pattern. Since in most engineering practices the idealized case is usually the best attainable result, some means of verification is in order at this point.

TABLE 1  
THE POWER GAIN OF THE MODEL ARRAY WITH  
RESPECT TO AN INDIVIDUAL ELEMENT

L	M	Field Max.	Reference Power	Array Power	Gain
0	0	6.18	39.3 mw	1.497 mw	26.3
0	-7	5.23	28.2 mw	.912 mw	30.9
-3	-4	9.47	92.5 mw	2.225 mw	41.6
-3	-6	8.83	80.4 mw	1.355 mw	59.2
-2	-2	7.27	54.5 mw	1.809 mw	30.1

Using linear superposition, the uncoupled gain with reference to a single element of any array is equal to the number of elements of the array. Now if for some spacing of a two element array, it can be shown that a gain greater than two is possible then one could more readily accept the coupled gain figures obtained for the 36 element array. Earlier, it was stated, that any general results obtained using crossed slots as antenna elements would hold equally well if crossed dipoles were the antenna element. Thus, it will suffice to show that the gain of a two element array of dipoles may be greater than two. This approach is used since the mutual impedance of two dipoles as a function of antenna length and spacing is tabulated in various texts.<sup>1,3</sup>

The simultaneous voltage equations for the two dipoles are

$$\begin{aligned} V_1 &= Z_{11}I_1 + Z_{12}I_2 \\ V_2 &= Z_{12}I_1 + Z_{22}I_2. \end{aligned} \tag{61}$$

Assuming identical elements yields,  $Z_{11} = Z_{22}$  and  $Z_{12} = Z_{21}$ . Also for simplicity let  $V_s = V_1 = V_2$ . Therefore  $I_s = I_1 = I_2$  and thus,

$$I_s = V_s / Z_s,$$

where

$$Z_s = Z_{11} + Z_{12}. \quad (62)$$

The total power to the two elements may be expressed as

$$P_T = \text{Re} \left[ V_1 I_1^* + V_2 I_2^* \right], \quad (63)$$

$$P_T = \text{Re} \left[ V_s \left[ \frac{V_s}{Z_s} \right]^* + V_s \left[ \frac{V_s}{Z_s} \right]^* \right],$$

or

$$P_T = 2 \frac{|V_s|^2}{|Z_s|^2} R_s, \quad (64)$$

where  $R_s$  is the real part of  $Z_s$ .

The field pattern of a dipole is proportional to the current distribution along the antenna, so the weighted array factor may be given as

$$F(\theta, \phi) = I_1 e^{-jk(r-r_1)} + I_2 e^{-jk(r-r_1)},$$

and

$$F(\theta, \phi)_{\max} = |I_1| + |I_2| = 2|I_s|,$$

or

$$F(\theta, \phi)_{\max} = 2 \frac{|V_s|}{|Z_s|}.$$

The input current to the reference dipole necessary to yield the same array factor maximum as the array is

$$I_{\text{ref}} = \frac{2|V_s|}{|Z_s|} \quad (65)$$

The input voltage to the reference antenna is given by

$$V_{\text{ref}} = \frac{2|V_s|}{|Z_s|} Z_{11}, \quad (66)$$

where  $Z_{11}$  is the self impedance of an isolated dipole.

The reference power is expressed as

$$P_{\text{ref}} = \text{Re} \left[ V_{\text{ref}} I_{\text{ref}}^* \right], \quad (67)$$

$$P_{\text{ref}} = \frac{2|V_s|}{|Z_s|} \left[ \frac{2|V_s|}{|Z_s|} R_{11} \right]$$

or

$$P_{\text{ref}} = \frac{4|V_s|^2}{|Z_s|^2} R_{11} \quad (68)$$

where  $R_{11}$  is the real part of  $Z_{11}$ .

From equations (68) and (64) one may directly obtain the gain of the array;

$$G = 2 \frac{R_{11}}{R_T} \quad (69)$$

or

$$G = 2 \frac{R_{11}}{R_{11} + R_{12}} \quad (70)$$

If the mutual coupling is assumed to be negligible then the gain is two. This corresponds to the number of elements. Also, if the gain is to be greater than two,  $R_{12}$  must be negative. Figure 9 shows that  $R_{12}$  may be negative for various spacings. Thus, the coupled gain of an antenna array may definitely be greater than that of the uncoupled case. This justifies the previously obtained result.

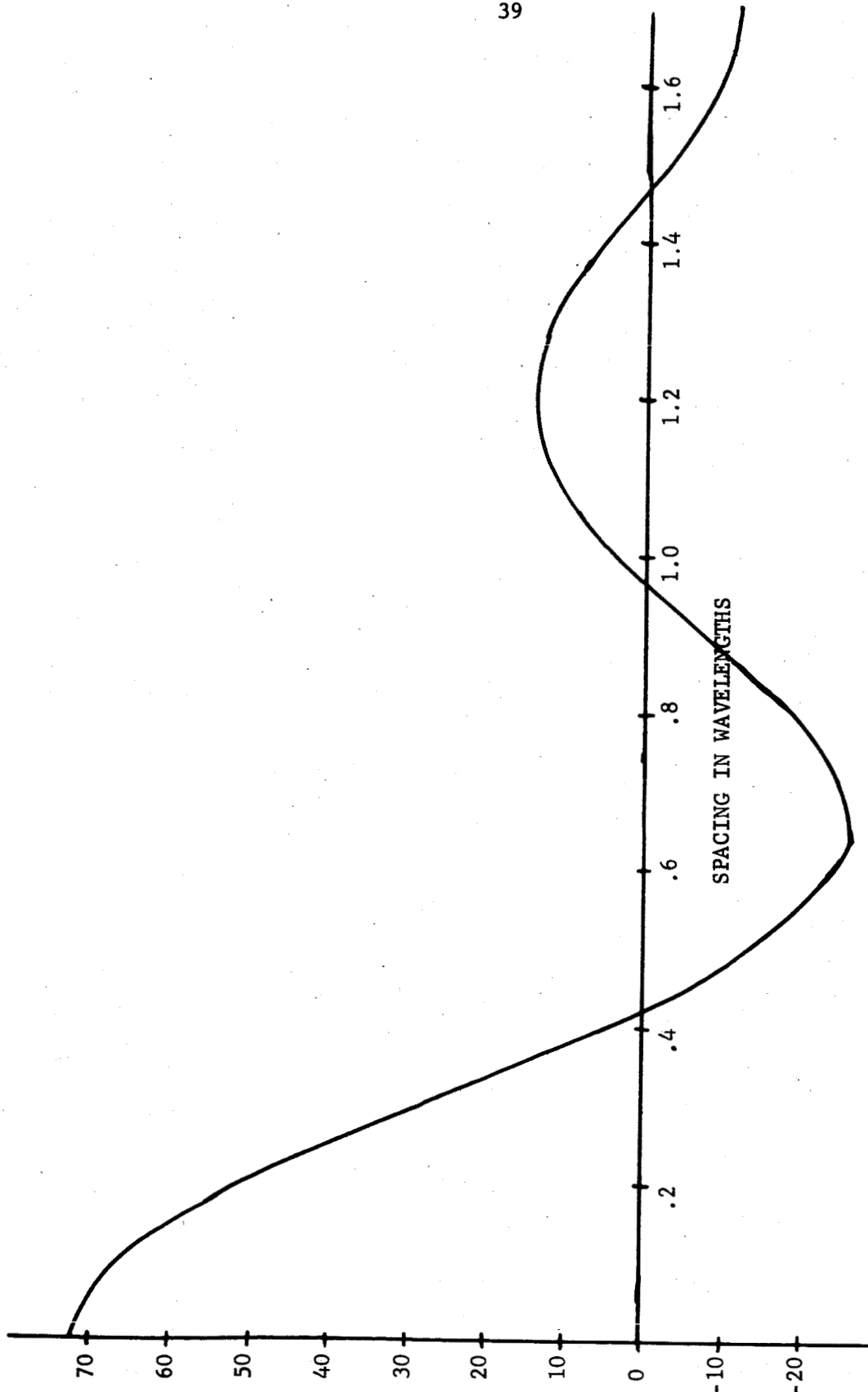


Fig. 9--The mutual resistance between two parallel dipoles of half length  $.250\lambda$ .<sup>3</sup>

#### IV. CONCLUSIONS

The array patterns obtained indicate that the array consists of enough elements such that many of the interior elements have essentially the same terminal admittance, and thus, produce the desired pattern. For smaller arrays this is not the case and the beam may not be properly steered. A four element array of crossed slots was briefly examined. The results definitely indicated an undesirable influence of mutual coupling on the array pattern.

The gain of the array was shown to vary throughout the hemisphere due to the coupling between elements. This variation of gain is normally not desirable. However, the worst case analyzed did not reduce the array gain more than two decibels with respect to the uncoupled case. This small variation may easily be tolerated. Thus, it may be concluded that the mutual coupling between the crossed slots will not significantly impair the scanning capabilities of the array.



#### BIBLIOGRAPHY

1. Kraus, John D., Antennas, McGraw-Hill Book Company, Inc., 1950, Chapter 10.
2. Fradin, A.Z., Microwave Antennas, Pergamon Press, 1961, Chapter 8.
3. Jasik, Henry, Antenna Engineering Handbook, McGraw-Hill Book Company, 1961, Chapter 3.

## APPENDIX A

The tabulated results of the solutions to the simultaneous equations representing the current and voltages of the slots are presented in this Appendix.

TABLE A-1

THE TERMINAL VOLTAGE AND ADMITTANCE OF THE 36 ELEMENT MODEL  
ARRAY OF PARALLEL SLOTS FOR L = 0 AND M = 0

ELEMENT pq	INPUT CURRENT		TERMINAL VOLTAGE		TERMINAL ADMITTANCE	
	Magn.	Phase	Magn.	Phase	Magn.	Phase
00	.25 ma	0.0°	.145 v	1.9	1.73 mmhos	-1.9
01	.25	0.0	.179	8.8	1.39	-8.8
02	.25	0.0	.164	10.7	1.52	-10.7
03	.25	0.0	.162	6.9	1.54	-6.9
04	.25	0.0	.174	15.3	1.43	-15.3
05	.25	0.0	.186	-5.7	1.34	5.7
10	.25	0.0	.180	8.8	1.39	-8.8
11	.25	0.0	.202	24.6	1.24	-24.6
12	.25	0.0	.178	22.7	1.41	-22.7
13	.25	0.0	.177	20.7	1.42	-20.7
14	.25	0.0	.199	25.4	1.25	-25.4
15	.25	0.0	.175	15.4	1.43	-15.4
20	.25	0.0	.164	10.5	1.52	-10.5
21	.25	0.0	.177	22.8	1.41	-22.8
22	.25	0.0	.161	17.1	1.55	-17.1
23	.25	0.0	.162	16.6	1.54	-16.6
24	.25	0.0	.177	20.5	1.41	-20.5
25	.25	0.0	.161	6.7	1.55	-6.7
30	.25	0.0	.160	7.1	1.56	-7.1
31	.25	0.0	.178	20.7	1.40	-20.7
32	.25	0.0	.162	16.3	1.55	-16.3
33	.25	0.0	.161	17.2	1.55	-17.2
34	.25	0.0	.177	22.5	1.41	-22.5
35	.25	0.0	.163	11.3	1.54	-11.3
40	.25	0.0	.178	17.5	1.41	-17.5
41	.25	0.0	.199	26.0	1.26	-26.0
42	.25	0.0	.177	20.4	1.42	-20.4
43	.25	0.0	.178	22.9	1.41	-22.9
44	.25	0.0	.202	24.7	1.24	-24.7
45	.25	0.0	.179	8.6	1.40	-8.6
50	.25	0.0	.189	-2.7	1.33	2.7
51	.25	0.0	.170	15.9	1.47	-15.9
52	.25	0.0	.163	6.4	1.53	-6.4
53	.25	0.0	.163	11.0	1.53	-11.0
54	.25	0.0	.180	8.7	1.39	-8.7
55	.25	0.0	.145	2.0	1.73	-2.0

TABLE A-2  
 THE TERMINAL VOLTAGE AND ADMITTANCE OF THE 36 ELEMENT MODEL  
 ARRAY OF PARALLELED SLOTS FOR L = 0 and M = -7

ELEMENT	INPUT CURRENT		TERMINAL VOLTAGE		TERMINAL ADMITTANCE	
	PQ	Magn. Phase	Magn. Phase	Magn. Phase	Magn. Phase	
00	.25 ma	0.0	.272 v	-37.4	.92 mmhos	37.4 <sup>o</sup>
01	.25	0.0	.235	-23.9	1.07	23.9
02	.25	0.0	.227	-28.2	1.10	28.2
03	.25	0.0	.232	-27.8	1.08	27.8
04	.25	0.0	.233	-31.6	1.07	31.6
05	.25	0.0	.181	-41.8	1.38	41.8
10	.25	-157.5	.211	152.2	1.19	50.3
11	.25	-157.5	.198	155.4	1.26	47.1
12	.25	-157.5	.198	160.7	1.26	41.9
13	.25	-157.5	.198	157.8	1.26	44.7
14	.25	-157.5	.201	155.1	1.25	47.4
15	.25	-157.5	.198	137.1	1.26	75.4
20	.25	-315.0	.169	-4.8	1.48	49.8
21	.25	-315.0	.143	-11.3	1.75	56.4
22	.25	-315.0	.150	-5.4	1.67	50.4
23	.25	-315.0	.156	-4.7	1.60	49.7
24	.25	-315.0	.157	-10.5	1.59	55.5
25	.25	-315.0	.176	-32.0	1.42	77.0
30	.25	-112.5	.142	-158.6	1.76	46.1
31	.25	-112.5	.110	-168.8	2.27	56.3
32	.25	-112.5	.104	-161.4	2.40	48.9
33	.25	-112.5	.115	-160.8	2.17	48.3
34	.25	-112.5	.128	-166.9	1.96	54.4
35	.25	-112.5	.153	165.9	1.63	81.6
40	.25	-270.0	.114	48.2	2.20	41.8
41	.25	-270.0	.089	41.8	2.80	48.2
42	.25	-270.0	.087	47.2	2.86	42.8
43	.25	-270.0	.087	52.2	2.87	37.8
44	.25	-270.0	.101	46.2	2.48	43.8
45	.25	-270.0	.131	12.8	1.90	77.2
50	.25	-67.5	.093	-93.7	2.70	26.2
51	.25	-67.5	.079	-93.2	3.16	25.7
52	.25	-67.5	.072	-96.3	3.45	28.8
53	.25	-67.5	.068	-94.6	3.66	27.1
54	.25	-67.5	.079	-87.4	3.18	19.9
55	.25	-67.5	.113	-127.7	2.21	60.2

TABLE A-3

THE TERMINAL VOLTAGE AND ADMITTANCE OF THE 36 ELEMENT MODEL  
 ARRAY OF PARALLEL SLOTS FOR L = -2 and M = -2

ELEMENT pq	INPUT CURRENT		TERMINAL VOLTAGE Coupled		TERMINAL ADMITTANCE	
	Magn.	Phase	Magn.	Phase	Magn.	Phase
00	.25 ma	0	.227 v	3.2	1.10 mmhos	-3.2
01	.25	-45	.227	-32.9	1.10	-12.1
02	.25	-90	.222	-83.4	1.13	-6.6
03	.25	-135	.224	-123.0	1.11	-12.0
04	.25	-180	.254	-175.8	0.98	-4.2
05	.25	-225	.198	121.5	1.26	13.5
10	.25	-45	.226	-32.8	1.11	-12.2
11	.25	-90	.182	-73.3	1.38	-16.7
12	.25	-135	.201	-120.3	1.24	-14.2
13	.25	-180	.201	-161.4	1.24	-18.5
14	.25	-225	.226	143.4	1.10	-8.4
15	.25	-270	.141	88.5	1.77	1.5
20	.25	-90	.221	-83.1	1.13	-6.9
21	.25	-135	.203	-120.3	1.23	-14.7
22	.25	-180	.220	-165.8	1.14	-14.2
23	.25	-225	.221	149.1	1.13	-14.1
24	.25	-270	.242	95.3	1.03	-5.3
25	.25	-315	.170	41.4	1.47	3.6
30	.25	-135	.222	-123.7	1.13	-11.3
31	.25	-180	.202	-161.1	1.23	-18.9
32	.25	-225	.227	149.0	1.09	-14.0
33	.25	-270	.218	106.6	1.14	-16.6
34	.25	-315	.233	50.6	1.07	-5.6
35	.25	0	.156	-5.0	1.60	5.0
40	.25	-180	.246	-176.4	1.01	-3.6
41	.25	-225	.231	143.8	1.08	-8.8
42	.25	-270	.239	95.9	1.05	-5.9
43	.25	-315	.231	50.3	1.08	-5.3
44	.25	0	.244	0.2	1.02	-.2
45	.25	-45	.162	-52.2	1.54	7.2
50	.25	-225	.195	125.3	1.28	9.7
51	.25	-270	.138	87.3	1.82	2.7
52	.25	-315	.171	41.4	1.46	3.6
53	.25	0	.156	-4.3	1.60	4.3
54	.25	-45	.161	-52.2	1.55	7.2
55	.25	-90	.115	-97.2	2.17	7.2

TABLE A-4  
 THE TERMINAL VOLTAGE AND ADMITTANCE OF THE 36 ELEMENT MODEL  
 ARRAY OF PARALLEL SLOTS FOR L = -3 and M = -4

ELEMENT	INPUT CURRENT		TERMINAL VOLTAGE		TERMINAL ADMITTANCE	
	pq	Magn. Phase	Magn. Phase	Magn. Phase	Magn. Phase	
00	.25 ma	0.0	.376 v	-12.0	.66 mmhos	12.0
01	.25	-67.5	.333	-78.2	.75	10.7
02	.25	-135.0	.357	-147.3	.70	12.3
03	.25	-202.5	.355	140.5	.70	17.0
04	.25	-270.0	.318	66.3	.79	23.7
05	.25	-337.5	.212	-5.6	1.18	28.1
10	.25	-90.0	.330	-100.6	.76	10.6
11	.25	-157.5	.316	-177.6	.79	20.1
12	.25	-225.0	.304	117.2	.82	17.8
13	.25	-292.5	.313	45.8	.80	21.7
14	.25	0.0	.283	-31.6	.88	31.6
15	.25	-67.5	.152	-110.2	1.64	42.7
20	.25	-180.0	.362	170.3	.69	9.7
21	.25	-247.5	.303	95.9	.83	16.6
22	.25	-315.0	.297	29.8	.84	15.2
23	.25	-22.5	.297	-39.0	.84	16.5
24	.25	-90.0	.268	-115.8	.93	25.8
25	.25	-157.5	.130	172.6	.19	29.9
30	.25	-270.0	.365	74.5	.68	15.5
31	.25	-337.5	.318	2.9	.79	19.6
32	.25	-45.0	.308	-60.8	.81	15.8
33	.25	-112.5	.306	-129.0	.82	16.5
34	.25	-180.0	.291	156.0	.86	24.0
35	.25	-247.5	.159	86.3	1.58	26.2
40	.25	0.0	.316	-21.8	.79	21.8
41	.25	-67.5	.276	-96.0	.91	28.5
42	.25	-135.0	.257	-159.9	.97	24.9
43	.25	-202.5	.274	135.7	.91	21.8
44	.25	-270.0	.268	60.2	.93	29.8
45	.25	-337.5	.160	-10.1	1.56	32.6
50	.25	-90.0	.199	-113.2	1.26	23.2
51	.25	-157.5	.156	175.8	1.60	26.7
52	.25	-225.0	.149	117.5	1.68	17.5
53	.25	-292.5	.166	53.6	1.51	13.9
54	.25	0.0	.172	-24.3	1.45	24.3
55	.25	-67.5	.098	-93.1	2.54	25.6

TABLE A-5  
 THE TERMINAL VOLTAGE AND ADMITTANCE OF THE 36 ELEMENT MODEL  
 ARRAY OF PARALLEL SLOTS FOR L = -3 and M = -6

ELEMENT pq	INPUT CURRENT		TERMINAL VOLTAGE Coupled		TERMINAL ADMITTANCE	
	Magn.	Phase	Magn.	Phase	Magn.	Phase
00	.25 ma	0.0	.39 v	-44.9°	.64	44.9°
01	.25	-67.5	.32	-117.0	.78	49.5
02	.25	-135.0	.33	177.0	.75	48.0
03	.25	-202.5	.32	108.1	.77	49.4
04	.25	-270.0	.29	39.5	.86	50.5
05	.25	-337.5	.20	-24.6	1.26	47.1
10	.25	-135.0	.36	174.5	.70	50.5
11	.25	-202.5	.34	100.8	.73	56.7
12	.25	-270.0	.32	31.6	.79	58.4
13	.25	-337.5	.31	-34.3	.80	56.8
14	.25	-45.0	.29	-103.5	.86	58.5
15	.25	-112.5	.19	-179.8	1.32	67.3
20	.25	-270.0	.34	43.9	.74	46.1
21	.25	-337.5	.33	-36.9	.77	59.4
22	.25	-45.0	.31	-104.9	.82	59.9
23	.25	-112.5	.29	-173.5	.87	61.0
24	.25	-180.0	.27	119.1	.94	60.9
25	.25	-247.5	.17	37.9	1.49	74.6
30	.25	-45.0	.32	-89.4	.78	41.4
31	.25	-112.5	.30	-169.0	.83	56.5
32	.25	-180.0	.29	120.5	.87	59.5
33	.25	-247.5	.26	51.3	.95	61.2
34	.25	-315.0	.24	-18.0	1.03	63.0
35	.25	-22.5	.14	-104.2	1.74	81.7
40	.25	-180.0	.28	146.4	.89	33.6
41	.25	-247.5	.24	63.0	1.02	49.5
42	.25	-315.0	.23	-8.8	1.10	53.8
43	.25	-22.5	.22	-77.6	1.16	55.1
44	.25	-90.0	.20	-147.9	1.25	57.9
45	.25	-157.5	.11	125.5	2.24	77.0
50	.25	-315.0	.19	24.7	1.29	20.3
51	.25	-22.5	.15	-45.9	1.61	23.4
52	.25	-90.0	.14	-115.1	1.75	25.1
53	.25	-157.5	.14	175.7	1.75	26.8
54	.25	-225.0	.14	102.8	1.73	32.2
55	.25	-292.5	.07	17.7	3.60	49.8

## APPENDIX B

The following figures illustrate the effect of mutual coupling on the array pattern of the 36 element model array.



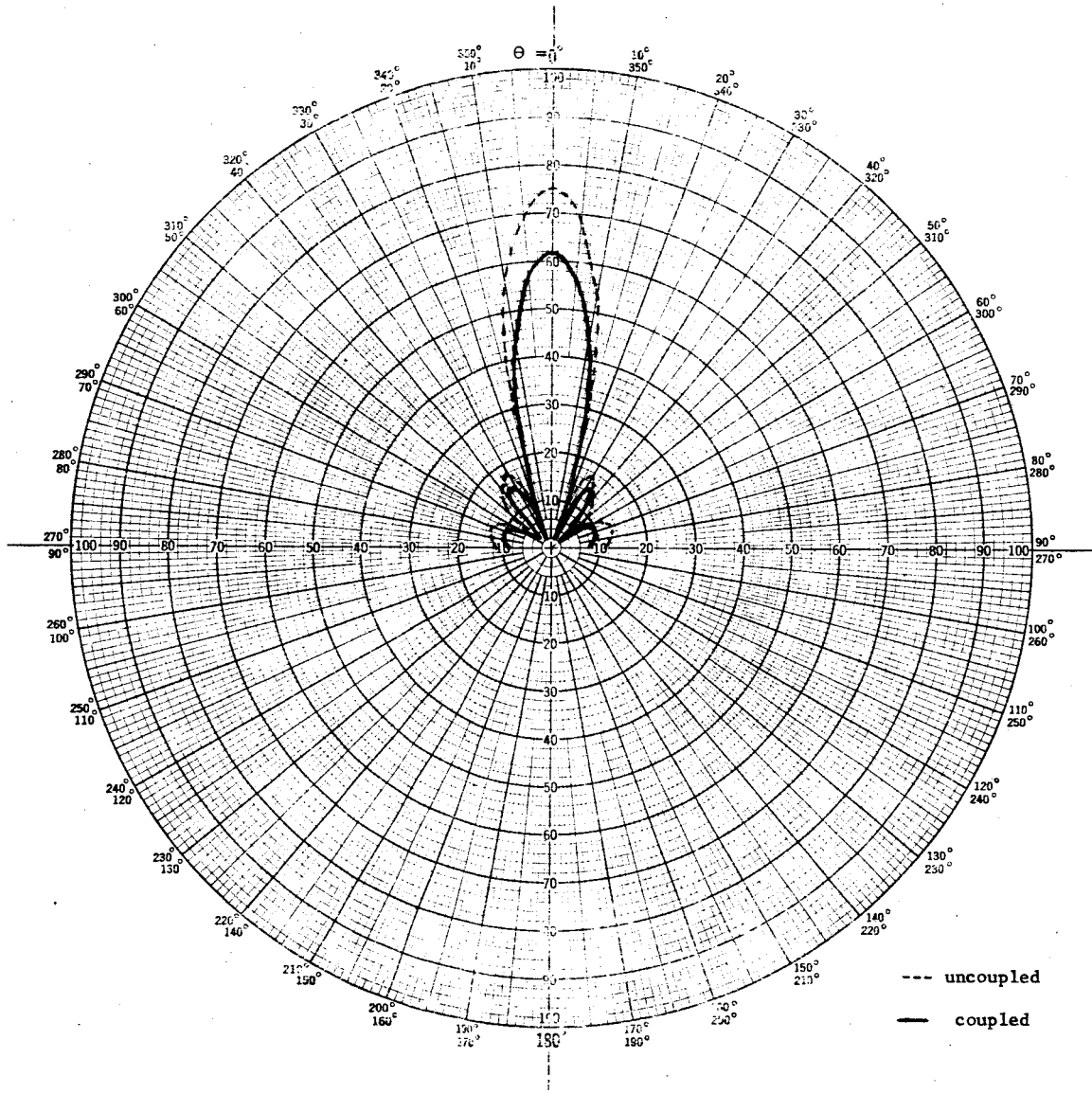


Fig. B-1--The elevation pattern for the 6 x 6 model antenna array with  $L = 0$ ,  $M = 0$ . ( $\phi = 90^\circ$ )

Polar Chart No. 127L  
SCIENTIFIC-ATLANTA, INC.  
ATLANTA, GEORGIA

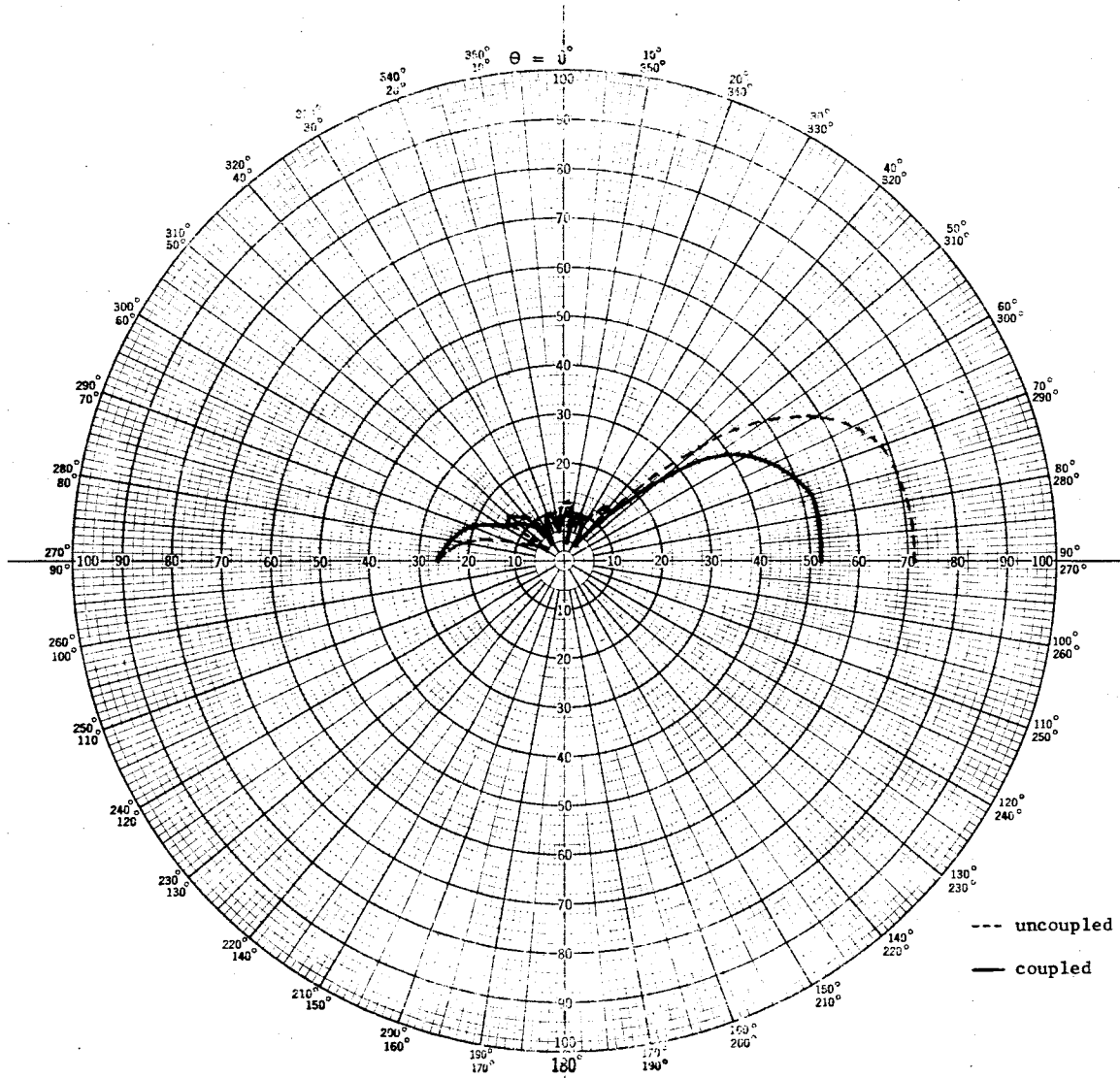


Fig. B-2--The elevation pattern for the 6 x 6 model antenna array with  $L = 0$ ,  $M = -7$ . ( $\phi = 90^\circ$ )

Polar Chart No. 127L  
SCIENTIFIC ATLANTA, INC.  
ATLANTA, GEORGIA

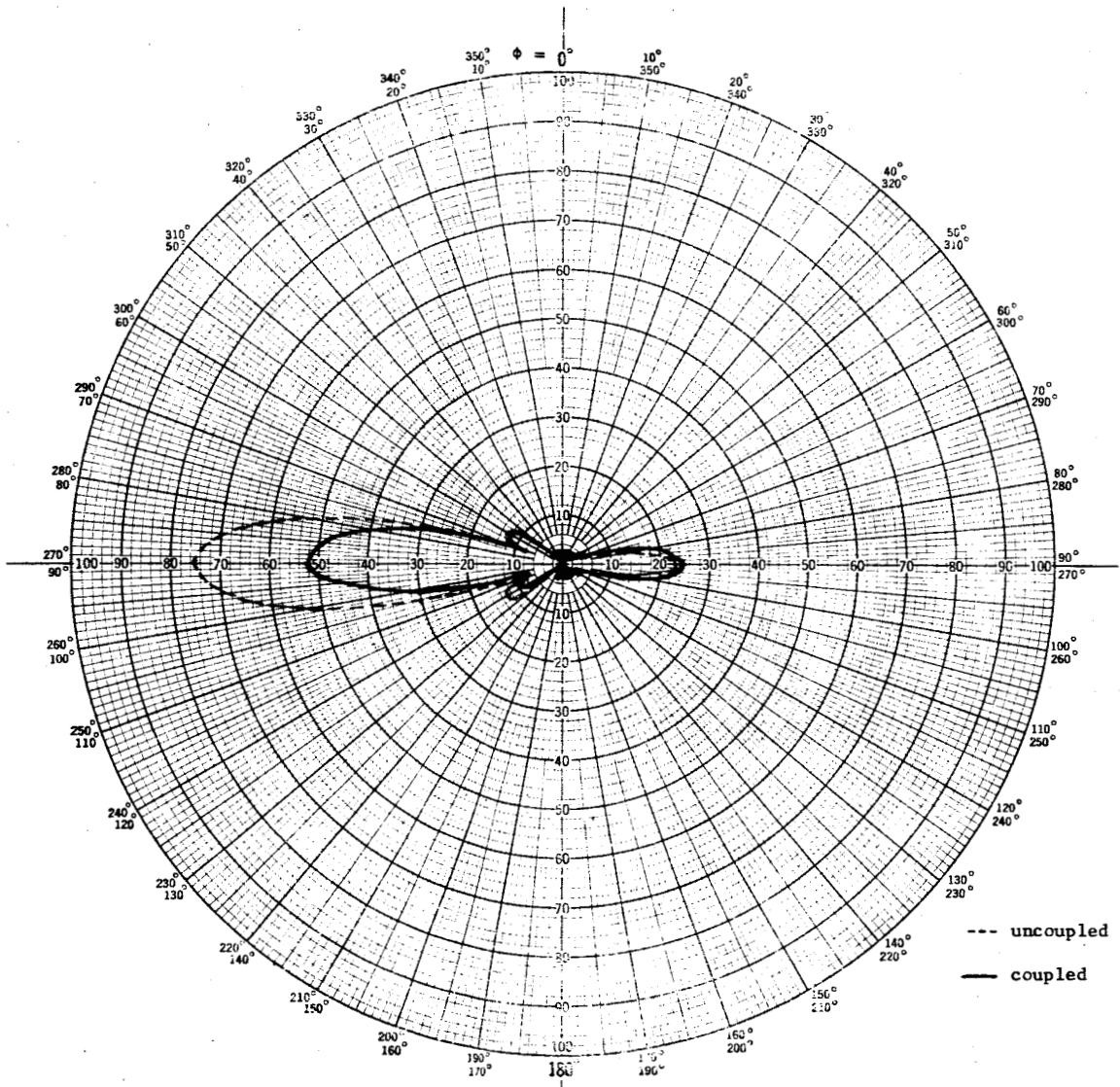


Fig. B-3--The azimuth array pattern for the 6 x 6 model antenna array with  $L = 0$ ,  $M = -7$ . ( $\Theta = 84^\circ$ )

Polar Chart No. 127.  
SCIENTIFIC-ATLANTA, INC.  
ATLANTA, GEORGIA



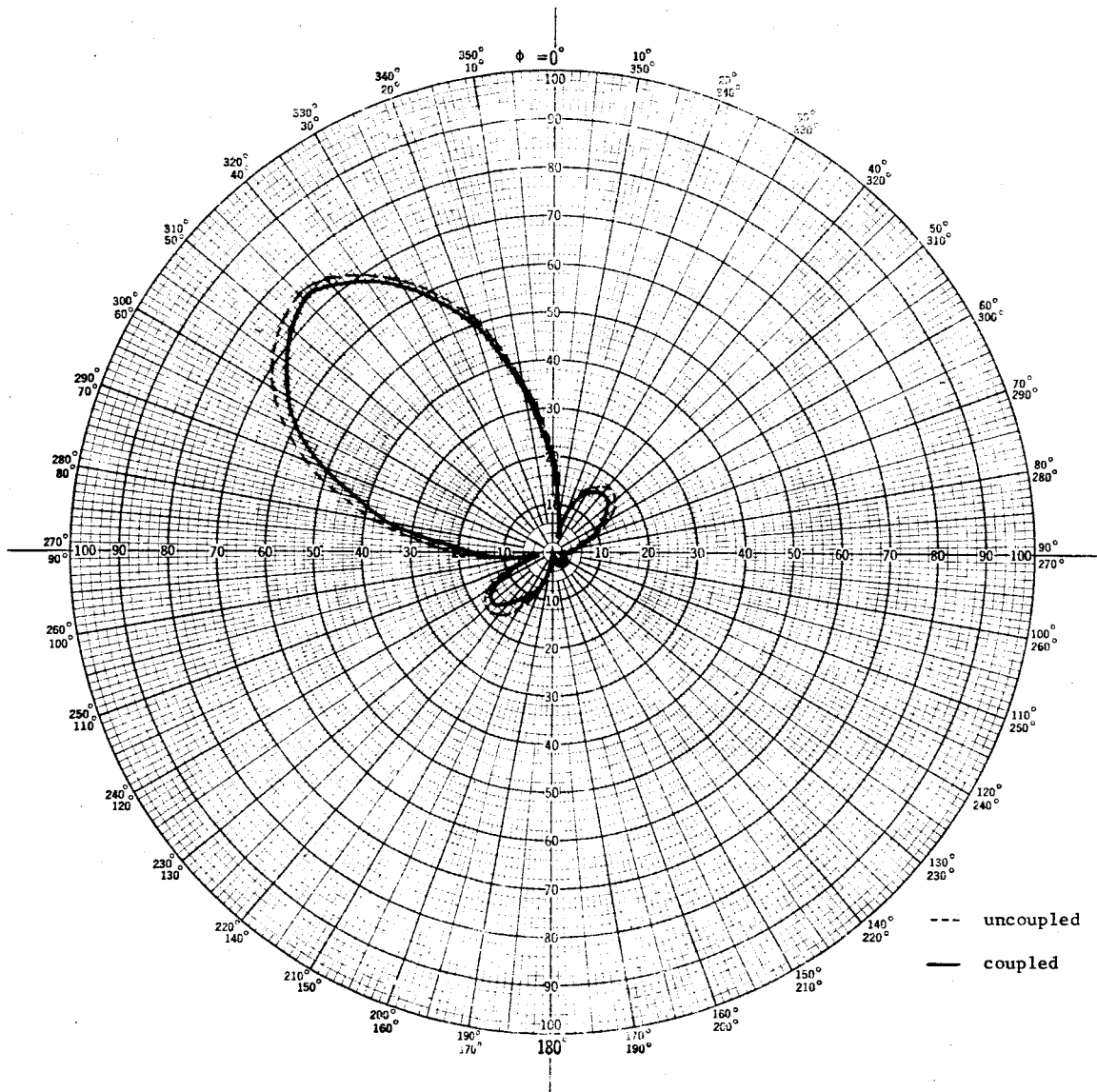


Fig. B-5--The azimuth array pattern for the 6 x 6 model antenna array with L = - 2, M = - 2. ( $\theta = 24^\circ$ )

Polar Chart No. 127L  
SCIENTIFIC-ATLANTA, INC.  
ATLANTA, GEORGIA

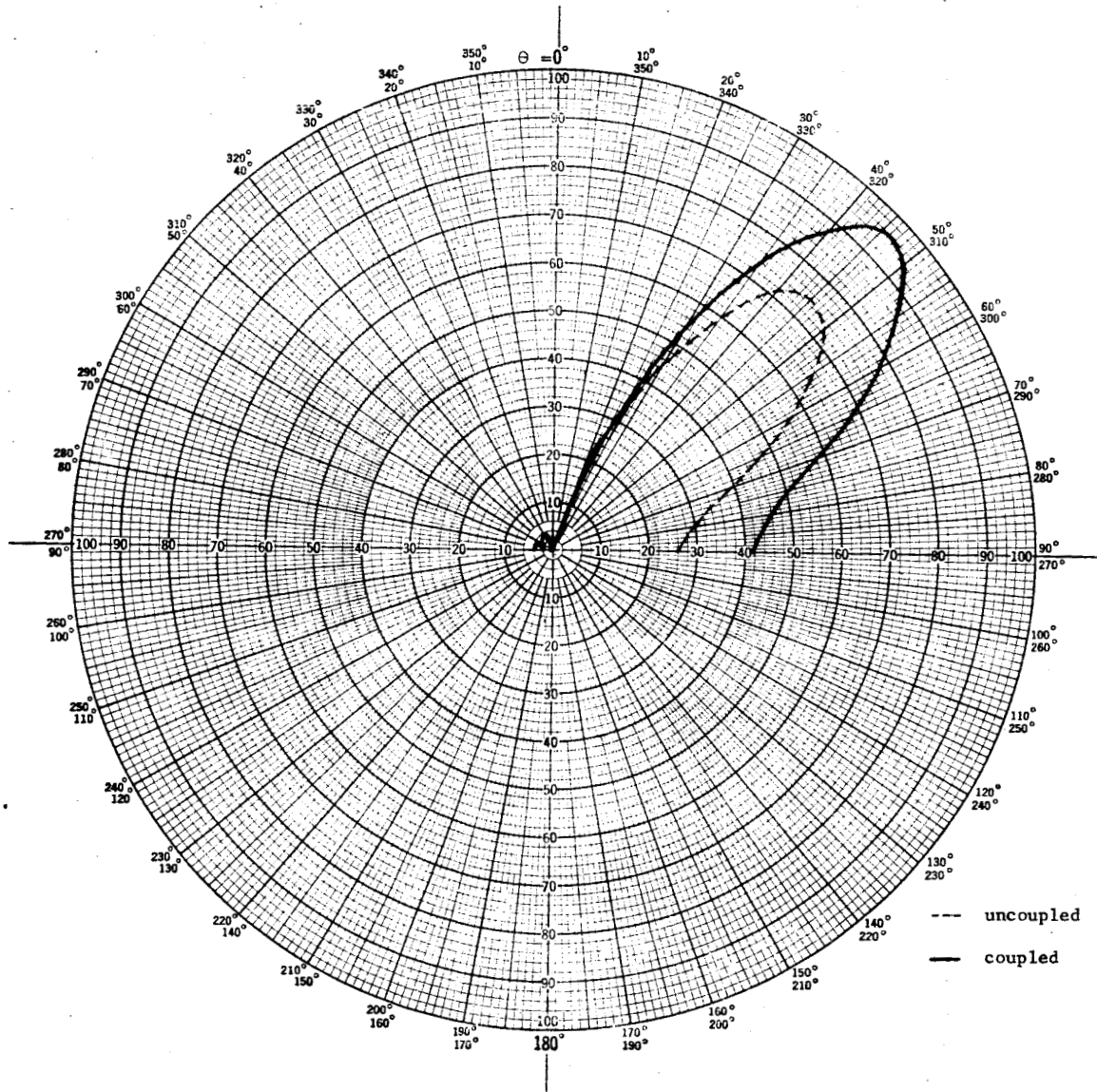


Fig. B-6--The elevation pattern for the 6 x 6 model antenna array with  $L = -3$ ,  $M = -4$ . ( $\phi = 53^\circ$ )

Polar Chart No. 127L  
 SCIENTIFIC-ATLANTA, INC.  
 ATLANTA, GEORGIA

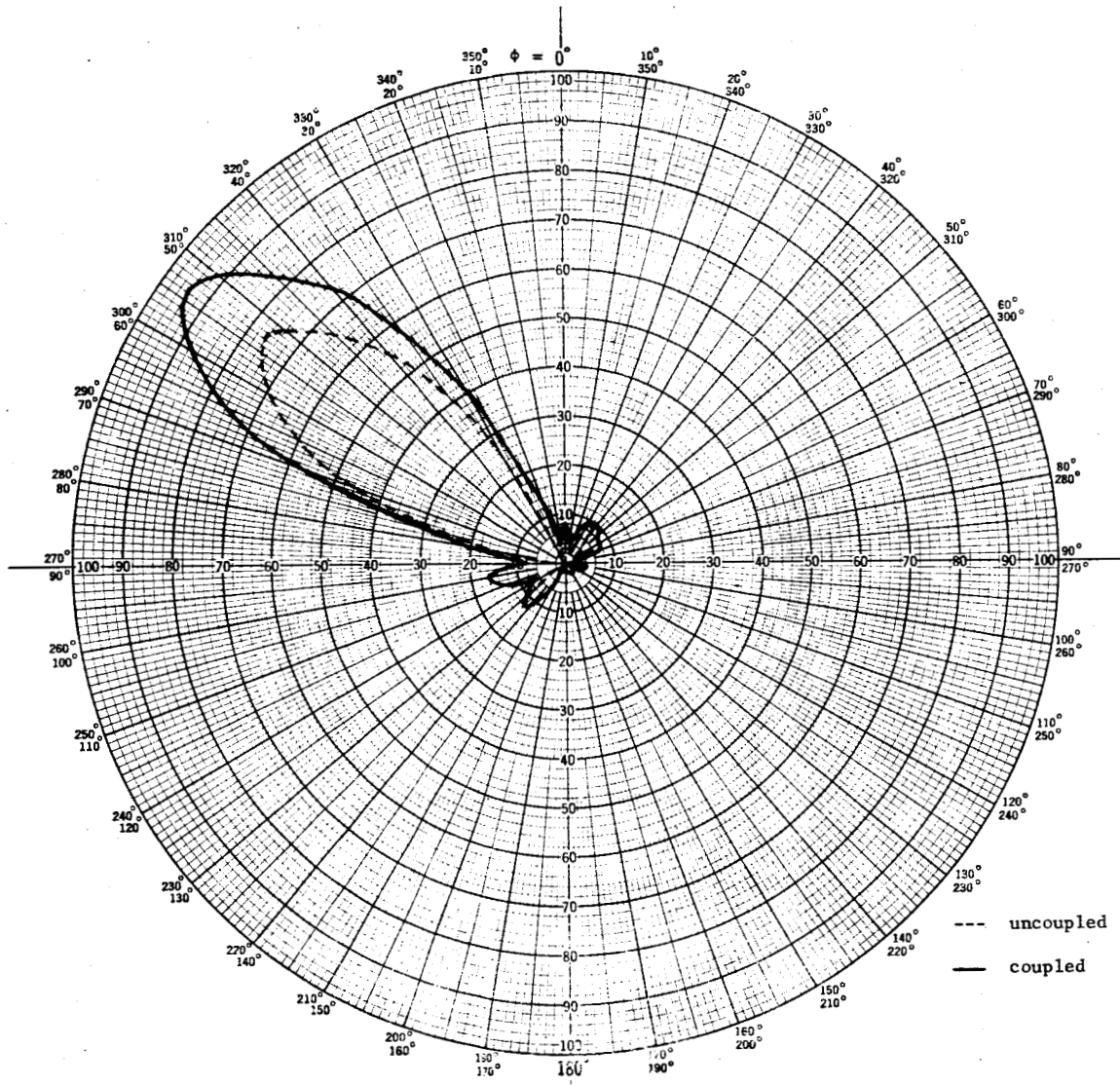


Fig. B-7--The azimuth array pattern for the 6 x 6 model antenna array with L = - 3, M = - 4. ( $\theta = 45^\circ$ )

Polar Chart No. 127L  
 SCIENTIFIC-ATLANTA, INC.  
 ATLANTA, GEORGIA

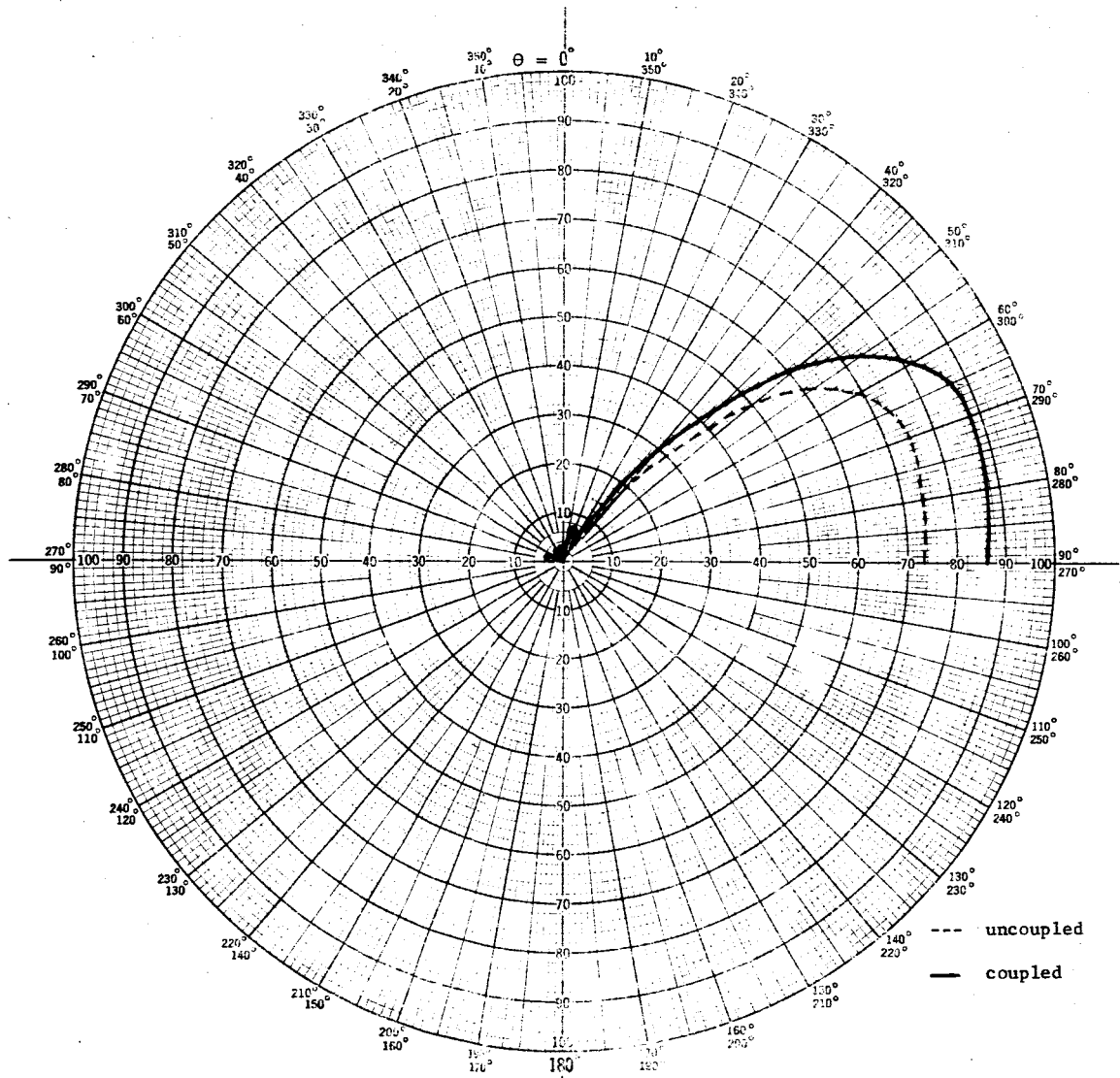


Fig. B-8--The elevation pattern for the 6 x 6 model antenna array with L = - 3, M = - 6. ( $\phi = 63^\circ$ )

Polar Chart No. 127L  
 SCIENTIFIC-ATLANTA, INC.  
 ATLANTA, GEORGIA



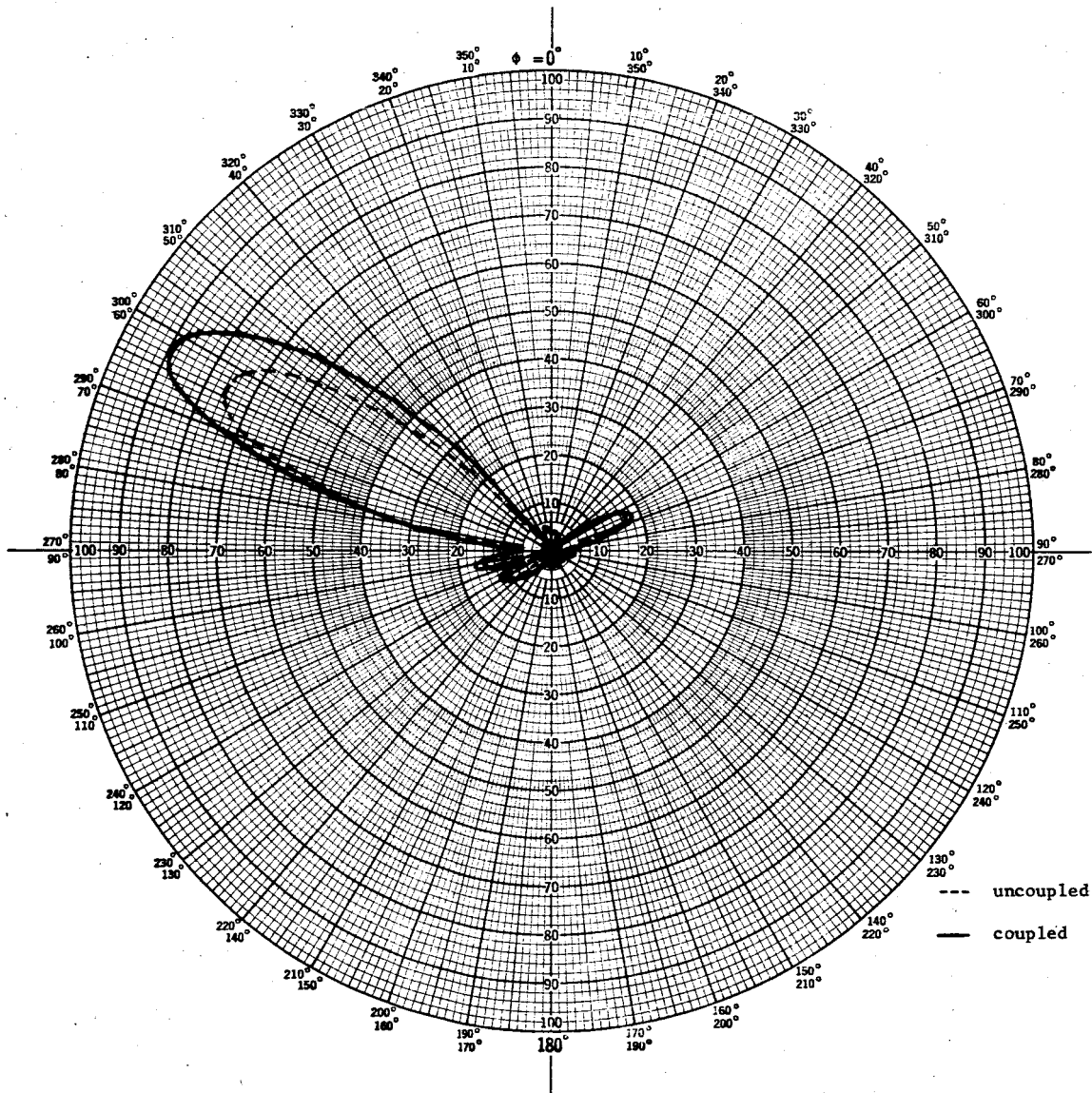


Fig. B-9--The azimuth array pattern for the 6 x 6 model antenna array with  $L = -3$ ,  $M = -6$ . ( $\theta = 72^\circ$ )

Polar Chart No. 127L  
SCIENTIFIC-ATLANTA, INC.  
ATLANTA, GEORGIA

## APPENDIX C

The following Fortran source programs were used to obtain the numerical results presented in the body of this report.

## SOURCE PROGRAM 1

### MUTUAL ADMITTANCE BETWEEN PARALLEL SLOTS

The following two programs yield the mutual admittances for all combinations of  $b$  and  $d$ , the quantities shown in Figure 2, that appear in the  $6 \times 6$  array of parallel slots. The input data to each program is the spacing between each element,  $SPACE$ , and the length of the slot,  $H$  in wavelengths. In these programs  $SPACE = .44$  and  $H = .5$ . The output yields  $G$ , where  $G$  is the real part of the mutual admittance, and  $S$ , the imaginary part, with  $b$  and  $d$  as parameters.

```

$JOB      074T
$TRJOB
$IRBTC
C      COMPUTATION OF MUTUAL ADMITTANCE BETWEEN SLOT ANTENNAS
C      SPACING=SPACE AND LENGTH=H
      READ 200,SPACE,H
      DIMENSION B(6,6),D(6,6)
      RT(D,B,Z)=SQRT(D**2+(B+H/2.-Z)**2)
      RB(D,B,Z)=SQRT(D**2+(B-H/2.-Z)**2)
      REEL(D,B,Z)=(SIN(6.2832*RT(D,B,Z))/RT(D,B,Z)+SIN(6.2832*
1      RB(D,B,Z))/RB(D,B,Z))*COS(6.2832*Z)
      UNREAL(D,B,Z)=(COS(6.2832*RT(D,B,Z))/RT(D,B,Z)+COS(6.2832*RB(D,B,
2      Z))/RB(D,B,Z))*COS(6.2832*Z)
      DO 10 I=1,6
      DO 10 J=1,6
      IF(I.GT.J) GO TO 10
      V=I-1
      W=J-I
      D(I,J)=W*SPACE/1.414214
      B(I,J)=D(I,J)+V*SPACE*1.414214
      N=8
3      K=0
      Z0=-H/2.
      Z1=Z0+H/2.**N
      Z2=Z1+H/2.**N
      SREAL=0.0
      SIMAG=0.0
5      SREAL=SREAL+REEL(D(I,J),B(I,J),Z0)+4.*REEL(D(I,J),B(I,J),Z1)
1      +REEL(D(I,J),B(I,J),Z2)
      SIMAG=SIMAG+UNREAL(D(I,J),B(I,J),Z0)+4.*UNREAL(D(I,J),B(I,J),Z1)
2      +UNREAL(D(I,J),B(I,J),Z2)
      Z0=Z2
      Z1=Z2+H/2.**N
      Z2=Z1+H/2.**N
      K=K+1
      IF(K.LT.2**(N-1)) GO TO 5
      G=H/(2.**N*3.)/(60.*9.8696044)*SREAL
      S=H/(2.**N*3.)/(60.*9.8696044)*SIMAG
      PRINT 300,I,J,D(I,J),B(I,J),G,S
10     CONTINUE
200     FORMAT (2E10.0)
300     FORMAT (1X,3HI =,I2,3X,3HJ =,I2,3X,3HD =,F5.2,3X,3HB =,F5.2,
2         3X,3HG =,E16.7,3X,3HS =,E16.7)
7      STOP
      END
$ENTRY
      .440      0.50
$IBSYS

```

```

$JOB 074T
$IBJOB
$IBFTC
C COMPUTATION OF MUTUAL ADMITTANCE BETWEEN SLOT ANTENNAS
C SPACING=SPACE AND LENGTH=H
READ 200,SPACE,H
DIMENSION B(6,6),D(6,6)
RT(D,B,Z)=SQRT(D**2+(B+H/2.-Z)**2)
RB(D,B,Z)=SQRT(D**2+(B-H/2.-Z)**2)
REEL(D,B,Z)=(SIN(6.2832*RT(D,B,Z))/RT(D,B,Z)+SIN(6.2832*
1 RB(D,B,Z))/RB(D,B,Z))*COS(6.2832*Z)
UNREAL(D,B,Z)=(COS(6.2832*RT(D,B,Z))/RT(D,B,Z)+COS(6.2832*RB(D,B,
2 Z))/RB(D,B,Z))*COS(6.2832*Z)
DO 10 I=1,6
DO 10 J=1,6
IF(I.GT.J) GO TO 10
V=I-1
W=J-I
R(I,J)=W*SPACE/1.414214
D(I,J)=B(I,J)+V*SPACE*.414214
N=8
J K=0
Z0=-H/2.
Z1=Z0+H/2.**N
Z2=Z1+H/2.**N
SREAL=0.0
SIMAG=0.0
5 SREAL=SREAL+REEL(D(I,J),B(I,J),Z0)+4.*REEL(D(I,J),B(I,J),Z1)
1 +REEL(D(I,J),B(I,J),Z2)
SIMAG=SIMAG+UNREAL(D(I,J),B(I,J),Z0)+4.*UNREAL(D(I,J),B(I,J),Z1)
2 +UNREAL(D(I,J),B(I,J),Z2)
Z0=Z2
Z1=Z2+H/2.**N
Z2=Z1+H/2.**N
K=K+1
IF(K.LT.2**(N-1)) GO TO 5
G=H/(2.**N*3.)/(60.*9.8696044)*SREAL
S=H/(2.**N*3.)/(60.*9.8696044)*SIMAG
PRINT 300,I,J,D(I,J),B(I,J),G,S
10 CONTINUE
200 FORMAT (2E10.0)
300 FORMAT (1X,3HI =,I2,3X,3HJ =,I2,3X,3HD =,F5.2,3X,3HB =,F5.2,
2 3X,3HG =,E16.7,3X,3HS =,E16.7)
7 STOP
END
$ENTRY .440 0.50
$IBSYS

```

SOURCE PROGRAM 2

THE SOLUTION OF THE SIMULTANEOUS CURRENT EQUATIONS FOR THE  
36 ELEMENT ARRAY OF PARALLEL SLOTS

The following program yields the voltage to each slot of the 36 element array of parallel slots. The input data for the program is C, where C is the currents applied to each slot, and Y, the mutual admittances calculated in the previous program. These quantities are read into the program in matrix form as shown in equation (51). The output gives the terminal voltage, V, and phase, PHASE, of each element in the array.

```

$JOB 074T HAYES
$TIME 25
$IBJOB
$IBFTC
C SOLUTION TO SIMULTANEOUS CURRENT EQUATIONS FOR
C A 36 ELEMENT MODEL ARRAY OF PARALLEL SLOTS
  DIMENSION Y(72,72),C(72,5)
  READ (5,100) C
  DO 5 I=1,72
  DO 5 J=1,72
  IF(J.LE.I) GO TO 4
  RFAD(5,200) Y(I,J)
  Y(I,J)=Y(I,J)*1.F4
  Y(J,I)=Y(I,J)*(-1)**(J-1)
  4 IF(I.EQ.J) Y(I,J)=0.4116429E+02
  5 CONTINUE
  DO 111 N=1,72
  SUMSQ=0.
  DO 110 NN=1,72
110 SUMSQ=Y(N,NN)**2+SUMSQ
  DO 112 NN=1,72
112 Y(N,NN)=Y(N,NN)/SQRT(SUMSQ)
  DO 111 NN=1,5
111 C(N,NN)=C(N,NN)/SQRT(SUMSQ)
  CALL MATINV (Y,72,C,5,DET)
  DO 13 J=1,5
  DO 13 I=1,72,2
  N=I+1
  V=SQRT(C(I,J)**2+C(N,J)**2)
  PHASE=ATAN2(C(N,J),C(I,J))*180./3.14159
  L=N/2
  13 WRITE(6,500) L,V,PHASE
100 FORMAT (6F10.0)
200 FORMAT(E16.7)
500 FORMAT(1X,12HELEMENT NO. ,I2,3X,3HV =,E16.7,3X,7HPHASE =,F10.5)
  STOP
  END
$ENTRY

```

### SOURCE PROGRAM 3

#### ARRAY FACTOR

This program may be used to plot the array pattern given in equation (54). This pattern may be plotted for any constant elevation or azimuth angle,  $T_1$  and  $P$  respectively. The input data includes the relative position of each element in rectangular coordinates,  $X(I)$ ,  $Y(I)$ ,  $Z(I)$ . The relative amplitude,  $T(I)$ , and phase,  $G(I)$ , of each element is also required, along with the wavelength of the propagated signal,  $C$ . The output yields the magnitude and relative phase of the array factor with the elevation and azimuth angles as parameters.



```

$JOB 074T
$TIME 10
$IRJOB
$IBFTC ARRAY
C CALCULATION FOR A GENERAL ARRAY PATTERN
C THE CASE FOR L=0, M=0
C DIMENSION X(100),Y(100),Z(100),T(100),G(100),G2(100)
C READ(5,10)DT,DP,C,N
10 FORMAT(3F10.0,I10)
C DT=3.14159/180.*DT
C DP=3.14159/180.*DP
7 F=0.
DO 30 I=1,N
C READ(5,30)X(I),Y(I),Z(I),T(I),G(I)
30 FORMAT(5F10.0)
C T1=3.14159/2.
31 P=0.
35 A=0.
C B=0.
DO 40 I=1,N
C D=X(I)*SIN(T1)*COS(P)+Y(I)*SIN(T1)*SIN(P)+Z(I)*COS(T1)
C G2(I)=3.14159/180.*G(I)
C S=G2(I)+2.*3.14159/C*D
C A=A+T(I)*COS(S)
40 B=B+T(I)*SIN(S)
C F=SQRT(A**2+B**2)
C ANG=ATAN2(B,A)
C T2=180./3.1415*T1
C ANG=180./3.1415*ANG
C P2=180./3.1415*P
C WRITE(6,50)T2,P2,F,ANG
50 FORMAT(1X,7HTHETA =,F8.2,2X,5HPHI =,F8.2,2X,
19HPATTERN =,F15.8,2X,7HANGLE =,F8.2)
C E=E+1.
C IF(E.GT.2000.)GO TO 70
C P=P+DP
C IF(P.LT.6.28317)GO TO 35
C T1=T1-DT
C IF(T1.LT.(-.02))GO TO 70
C GO TO 31
70 STOP
END
$FNTRY
$IBSYS

```

SOURCE PROGRAM 4

THE INPUT POWER TO THE 36 ELEMENT  
ARRAY OF PARALLEL SLOTS

This program sums the power radiated by each element of the array to obtain the total radiated power. The input data is C, where C is the current applied to each element, and V, the calculated terminal voltage of each slot. The program yields the magnitude and phase of the terminal admittance,  $Y_M$  and  $Y_A$ , respectively, along with the total radiated power of the array.

```
$JOB 074T HAYES
$IBJOB
$IBFTC
C TERMINAL ADMITTANCE AND TOTAL INPUT POWER TO ARRAY FOR SPECIFIED
C POINTINGS
DIMENSION C(72,5),V(72,5)
READ 200,C
DO 5 J=1,5
DO 5 I=1,72
5 C(I,J)=C(I,J)*.25E-4
READ 300,V
DO 12 J=1,5
POW=0.0
DO 10 I=1,72,2
N=I+1
L=N/2
YM=SQRT((C(I,J)**2+C(N,J)**2)/(V(I,J)**2+V(N,J)**2))
YA=(ATAN2(C(N,J),C(I,J))-ATAN2(V(N,J),V(I,J)))*180./3.1415927
PM=YM*(V(I,J)**2+V(N,J)**2)
PA=3.1415927/180.*YA
POW=POW+PM*COS(PA)
10 WRITE(6,400)L,YM,YA
12 WRITE(6,500)J,POW
200 FORMAT(6F10.0)
300 FORMAT(6E12.7)
400 FORMAT(1X,12HELEMENT NO. ,I2,6X,3HY =,F16.7,3X,7HPHASE =,F12.4)
500 FORMAT(1X,9HCASE NO. ,I1,3X,3HL =,5X,3HM =,5X,13HTOTAL POWER =,
1 E16.7)
STOP
END
$ENTRY
```